Gaseous, $PM_{2.5}$ Mass, and Speciated Emission Factors from Laboratory Chamber Peat Combustion

John G. Watson[1,2*], Junji Cao[2,3], L.-W. Antony Chen[4], Qiyuan Wang[2], Jie Tian [2,3], Xiaoliang Wang[1], Steven Gronstal[1], Steven Sai Hang Ho[5], Adam C. Watts[1], Judith C. Chow[1,2]

[1]Division of Atmospheric Sciences, Desert Research Institute, Reno, Nevada, USA

[2]Key Laboratory of Aerosol Chemistry and Physics, Institute of Earth Environment, Chinese Academy of Sciences, Xi'an, China.

[3]CAS Center for Excellence in Quaternary Science and Global Change, Xi'an, China

[4]Department of Environmental and Occupational Health, University of Nevada, Las Vegas, Nevada, USA

[5]Hong Kong Premium Services and Research Laboratory, Hong Kong, China

Re-submitted to

Atmospheric Chemistry and Physics Discussion

Date

10 September 2019

[*]Corresponding Author: john.watson@dri.edu

Abstract

Peat fuels representing four biomes of boreal (western Russia and Siberia), temperate (northern Alaska, U.S.A.), subtropical (northern and southern Florida, U.S.A), and tropical (Borneo, Malaysia) regions were burned in a laboratory chamber to determine gas and particle emission factors (EFs). Tests with 25 % fuel moisture were conducted with predominant smoldering combustion conditions (average modified combustion efficiency [MCE] = 0.82 ± 0.08). Average fuel-based EF_{CO_2} (carbon dioxide) are highest (1400 ± 38 g kg^{-1}) and lowest (1073 ± 63 g kg^{-1}) for the Alaskan and Russian peats, respectively. EF_{CO} (carbon monoxide) and EF_{CH_4} (methane) are ~12–15 % and ~0.3–0.9 % of EF_{CO_2}, in the range of 157–171 g kg^{-1} and 3–10 g kg^{-1}, respectively. EFs for nitrogen species are at the same magnitude of EF_{CH_4}, with an average of 5.6 ± 4.8 and 4.7 ± 3.1 g kg^{-1} for EF_{NH_3} (ammonia) and EF_{HCN} (hydrogen cyanide); 1.9 ± 1.1 g kg^{-1} for EF_{NOx} (nitrogen oxides); as well as 2.4 ± 1.4 and 2.0 ± 0.7 g kg^{-1} for EF_{NOy} (total reactive nitrogen) and EF_{N_2O} (nitrous oxide).

An oxidation flow reactor (OFR) was used to simulate atmospheric aging times of ~2 and ~7 days to compare fresh (upstream) and aged (downstream) emissions. Filter-based $EF_{PM_{2.5}}$ varied by >4-fold (14–61 g kg^{-1}) without appreciable changes between fresh and aged emissions. The majority of $EF_{PM_{2.5}}$ consists of EF_{OC} (organic carbon), with $EF_{OC}/EF_{PM_{2.5}}$ ratios in the range of 52–98 % for fresh emissions, and ~15 % degradation after aging. Reductions of EF_{OC} (~7–9 g kg^{-1}) after aging are most apparent for boreal peats with the largest degradation in low temperature OC1 that evolves at <140°C, indicating the loss of high vapor pressure semi-volatile organic compounds upon aging. The highest $EF_{Levoglucosan}$ is found for Russian peat (~16 g kg^{-1}), with ~35-50 % degradation after aging. EFs for water-soluble OC (EF_{WSOC}) accounts for ~20–62 % of fresh EF_{OC}.

The majority (>95 %) of the total emitted carbon is in the gas phase with 54–75 % CO_2, followed by 8-30 % CO. Nitrogen in the measured species explains 24–52 % of the consumed fuel nitrogen with an average of 35 ± 11 %, consistent with past studies that report ~one- to two-thirds of the fuel nitrogen measured in biomass smoke. The majority (>99 %) of the total emitted nitrogen is in the gas phase, with an average of 16.7 % as NH_3 and 9.5 % as HCN. N_2O and NO_y constituted 5.7 % and 2.9 % of consumed fuel nitrogen. EFs from this study can be used to refine current emission inventories.

53 Keywords: Peat combustion, modified combustion efficiency, emission factors, oxidation flow
54 reactor, carbon balance, nitrogen budget.

1 Introduction

Globally, peatlands occupy ~3 % of the Earth's land surface, but they store as much as 610 gigatonnes (i.e., 610×10^{15} grams) of carbon, representing 20–30 % of the planet's terrestrial carbon (Page et al., 2011;Rein et al., 2009). Peatland fires can persist for weeks to months and are dominated by the smoldering-phase as opposed to the flaming-phase of biomass burning (Hu et al., 2018;Stockwell et al., 2016). This results in lower combustion efficiencies, increased particulate matter (PM) emissions, and larger fractions of brown carbon (BrC) compared to black carbon (BC) or soot (Pokhrel et al., 2016). Peat fires emit reduced nitrogen compounds (e.g., ammonia [NH_3] and hydrogen cyanide [HCN]); volatile and semi-volatile organic compounds (VOCs and SVOCs); and $PM_{2.5}$ (PM with aerodynamic diameters <2.5 μm) (Akagi et al., 2011;Yokelson et al., 2013). Peat smoke and ash affect ecosystem productivity, soil acidity, biogeochemical cycling, atmospheric chemistry, Earth's radiation balance, and human health. Warmer climates lower the water table in peatlands and change the pattern, frequency, and intensity of the peatland fires causing local- and regional-scale air pollution and visibility impairment (Page et al., 2002;Turetsky et al., 2010;2015a;2015b). For Southeast Asia, fire-related regional air pollution and its effects on atmospheric visibility, ecosystems, and human health have been addressed in many studies (e.g., Behera et al., 2014;Betha et al., 2013;Bin Abas et al., 2004;Dall'Osto et al., 2014;Engling et al., 2014;Fujii et al., 2017;Heil and Goldammer, 2001;Hu et al., 2019;Kundu et al., 2010;Levine, 1999;Tham et al., 2019).

Nitrogen, one of the most important plant nutrients, affects global carbon and biogeochemical cycles (Crutzen and Andreae, 1990;Gruber and Galloway, 2008). Deposition of oxidized and reduced nitrogen species from biomass burning, such as gaseous nitric oxide (NO), nitrogen dioxide (NO_2), and NH_3 as well as particulate nitrate (NO_3^-) and ammonium (NH_4^+), alters terrestrial ecosystems (Chen et al., 2010), while nitric acid (HNO_3) contributes to soil acidification and excessive nitrification that reduce plant resistance to environmental stresses (Goulding et al., 1998). Gaseous nitrogen oxides (NO_x) affect atmospheric chemistry through: 1) reactions with hydroxyl (OH) and peroxy ($HO_2 + RO_2$) radicals; 2) conversion to nitrate radical (NO_3), dinitrogen pentoxide (N_2O_5), and acyl peroxy nitrates (particularly peroxyacetyl nitrate [PAN]), which are important NO_x reservoirs; and 3) formation of ozone (O_3) and secondary organic aerosols (SOA) (Alvarado et al., 2010;Cubison et al., 2011;Ng et al., 2007). While NH_3 neutralizes HNO_3 to form particulate ammonium nitrate (NH_4NO_3), it may also react with alkanoic acids to form alkyl

amides, nitriles, and ammonium salts that can also contribute to SOA formation (Na et al., 2007;Simoneit et al., 2003;Zhao et al., 2013). In addition, NH_3 interacts with SOA to form "BrC" that further influence the aerosol radiative forcing (Updyke et al., 2012).

This study quantifies peat burning emission factors (EFs) for fresh and aged multipollutant mixtures through controlled burns in a laboratory combustion chamber with atmospheric aging simulated by an oxidation flow reactor (OFR). These tests are applied to peat samples from diverse parts of the world.

2 Experiment

2.1 Fuel types

Peatlands are found all over the world, as illustrated in Fig. 1 (based on Yu et al., 2010) with large deposits found in the northern USA and Canada, northern Europe, Russia/Siberia, and southeast Asia. Eight types of peat fuels from different regions and climates were collected for testing, including: boreal (i.e., Odintsovo, Russia and Pskov, Siberia); temperate (i.e., black spruce forest, northern Alaska, USA); subtropical (i.e., northern [Putnam County Lakebed] and southern [Everglades National Park] Florida, USA and Caohai and Gaopo, Guizhou, southwest China); and tropical (i.e., Borneo, Malaysia) peats.

Representative peat samples of 250–1150 g from the upper 20 cm of the peatland surface were excavated for each region indicated in Fig. 1. As peat is a heterogeneous mixture of decomposed plant material, it can be formed in different wetlands under changing climates and nutrient contents (Turetsky et al., 2015a). Supplemental Fig. S1 shows that the appearance of peat fuels varies by region.

To quantify carbon (C), hydrogen (H), nitrogen (N), sulfur (S), and oxygen (O) content, ~2–3 g of each peat fuel were dried in a vacuum oven (~105°C) for two hours prior to elemental analysis (Thermo Flash-EA 1112 CHNS/O Analyzer, Waltham, MA, USA).

Import and export regulations (USDA, 2010) require high temperature heating of soil/peat fuels as part of the sterilization process. Peat fuels were heated to 90°C and weighed every 24 hours to achieve a stable dry mass with ~0.16 % moisture by weight content (after ~96 hours of heating). The low heating temperature (i.e., below the water boiling point) minimized VOC losses, although some compounds with high volatilities could have been removed at 90°C. To better simulate the field conditions during peat fires, distilled-deionized water (DDW) was added to rehydrate the dry peat and achieve a fuel moisture of ~25 % (by weight) before each experiment

(Yatavelli et al., 2017). To examine the effects of fuel moisture on emissions, additional experiments (n=3) were conducted at 60 % fuel moisture content (by weight) for the Putnam (FL) peat.

2.2 Experimental setup

The laboratory setup shown in Fig. 2 used a biomass combustion chamber with a volume of ~8 m^3 (1.8 m[W] x 1.8 m[L] x 2.2 m[H]) (Tian et al., 2015). Instrument specifications and operating principles are shown in Table S1. The chamber is made of 3 mm-thick aluminum to withstand high temperature heating. A blower supplied air filtered by a charcoal bed and a high-efficiency particulate air (HEPA) filter near the bottom of the chamber to remove background gas and particle contaminants. The ventilation rate was controlled by the blower and exhaust fan at ~2.65 m^3 min^{-1}, resulting in a smoke residence time of ~ 3 min in the chamber assuming a well-stirred flow model.

For each test, ~10–30 g of dried peat was placed in an asbestos insulated circular container on top of an induction heater that provided heating during the first ~5–10 minutes of combustion (see Fig. S2). This method replaced a propane torch used in initial test burns, thereby minimizing non-peat burning emissions. The smoldering process is usually self-propagating and sustained by heat conduction and radiation with fuel mass continuously monitored by a scale underneath the induction heater (Ohlemiller et al., 1979).

Continuous $PM_{2.5}$ mass concentrations were monitored with a DustTrak (TSI Model 8532, Shoreview, MN, USA) (Wang et al., 2009) (Table S1). When $PM_{2.5}$ concentrations reached their maximum and started to decline, the induction heater was turned off. The fuel was consumed with diminished smoke emissions after ~20 minutes. Preliminary tests were conducted using ~10–20 g of fuel and a dilution ratio of ~3 to 5, yielding sufficient particle loadings on the filters (~150–290 μg per 47 mm filter disc). To achieve higher filter deposits of 300–600 μg per filter that accommodate comprehensive organic speciation, additional fuels (~15–20 g) were added with the induction heater turned on for another ~10 minutes. Sampling continued until the concentrations returned to background level.

Sampling ports for stack concentrations of carbon dioxide (CO_2) and multiple gases by Fourier transform infrared (FTIR; Model DX 4015; Gasmet Technologies Oy, Finland) spectroscopy were located ~1 m above the top of the chamber roof in the exhaust duct (Fig. 2). The FTIR spectrometer measured gaseous emissions prior to dilution to obtain enhanced signal-

to-noise ratios for trace gases (Jaakkola et al., 1998). An exhaust gas sample was drawn into the FTIR where the infrared (IR) absorption spectra in the wave number range of 900–4200 cm^{-1} were measured. The instrument software compares the measured absorption spectra with reference gas absorption spectra in the calibration library to identify gas species and calculate concentrations. Examples of reference gas spectra and an Everglades (FL) peat sample spectrum are plotted in Fig. S3.

Smoke from the chamber was drawn through a dilution sampling manifold where the exhaust was diluted with clean air to achieve cooling that allowed for condensation of SVOCs. A portion of the exhaust was directed through a potential aerosol mass (PAM)-OFR (Aerodyne Research Inc., Billerica, MA, USA) to simulate atmospheric aging prior to quantification by the sampling instruments shown in Fig. 2. The 185 and 254 nm (OFR185) ultraviolet (UV) lamps in the OFR were operated at 2 and 3.5 volts with 10 L min^{-1} flow rate to simulate intermediate-aged (~2 days) and well-aged (~7 days) emissions assuming an average daily OH concentration of 1.5 x 10^6 molecules cm^{-3}. The estimated OH exposures (OH_{exp}) at 2 and 3.5 volts were 2.6 x 10^{11} and 8.8 x 10^{11} molecules-sec cm^{-3} based on the measured decay of sulfur dioxide (SO_2) (Cao et al., 2019). Due to external OH reactivity from carbon monoxide (CO), NO_x, and other reactants, these OH_{exp} levels represent upper limits of the actual OH exposures inside the OFR (Li et al., 2015;Peng et al., 2015).

Oxides of nitrogen were measured as NO_x (the sum of NO and NO_2) and total reactive nitrogen (NO_y, including NO, NO_2, N_2O_5, HNO_3, HNO_4, $ClONO_2$, HONO, alkyl nitrates, and PAN) by chemiluminescence NO_x and NO_y analyzers (Allen et al., 2018;Ballenthin et al., 2003). The NO_x analyzers placed upstream and downstream of the OFR determined NO_x changes with OH_{exp} in the OFR. There are known interferences for the non-selective catalytic converter in the chemiluminescent NO_x analyzer and for spectroscopic absorption in the FTIR (Allen et al., 2018;Prenni et al., 2014;Villena et al., 2012). The chemiluminescence monitor converts most nitrogenous compounds to NO, with HNO_3 and PAN being the most important potential interferents (Winer et al., 1974). However, much of the available HNO_3 and PAN is removed by the tubing leading to the molybdenum converter in the standard NO_x analyzer, which is why the NO_y analyzer locates the converter at the inlet. Allen et al. (2018) found no significant differences between NO_x measurements of biomass burning plumes when comparing a chemiluminescent analyzer with more specific UV absorption measurements.

The following analyses are based on: 1) the commercial NO_x analyzers for NO, NO_2, and NO_x (NO + NO_2 as equivalent NO_2); 2) the NO_y analyzer for total reactive nitrogen; and 3) the FTIR spectrometer for trace gas measurements of methane (CH_4), NH_3, HCN, nitrous oxide (N_2O), and 13 low molecular-weight VOCs (C2–C6).

$PM_{2.5}$ filter packs were sampled upstream and downstream of the OFR to characterize fresh and aged emissions, respectively, with Minivol $PM_{2.5}$ samplers (Airmetrics, Springfield, OR, USA) operated at 5 L Min^{-1} flow rate per channel. $PM_{2.5}$ mass, elements, carbon, water-soluble organic carbon (WSOC), ions, carbohydrates, organic acids, as well as gaseous NH_3 and HNO_3 were obtained from the paired upstream and downstream filter samples to examine changes in speciated EFs and source profiles with photochemical aging. Average filter-based EFs are examined by peat types and aging times (i.e., denoted as Fresh 2 vs. Aged 2 and Fresh 7 vs. Aged 7) (Chow et al., 2019).

2.3 Filter pack measurements

$PM_{2.5}$ mass and major chemical species concentrations were obtained from the parallel Teflon-membrane and quartz-fiber filters (Teflo©, 2 μm pore size, R2PJ047 and Tissuquartz 2500 QAFUP, Pall Life Sciences, Port Washington, NY, USA). Teflon-membrane filters were equilibrated in a temperature (20–23°C) and relative humidity (30–40 %) controlled environment for a minimum of 48 hours prior to gravimetric analysis by a microbalance with ± 1 μg sensitivity (Watson et al., 2017). This was followed by multielemental analysis by x-ray fluorescence (Watson et al., 1999). Quartz-fiber filters were pre-fired at 900° C for four hours to minimize organic artifacts. A portion (0.5 cm^2) of the quartz-fiber filter was submitted for organic, elemental, and brown carbon (OC, EC, and BrC) analysis following the IMPROVE_A thermal/optical reflectance (TOR) protocol (Chow et al., 2007;2015). Half of the quartz-fiber filters was extracted in DDW for ionic speciation (i.e., chloride [Cl^-], nitrate [NO_3^-], nitrite [NO_2^-], sulfate [$SO_4^=$], water-soluble sodium [Na^+] and potassium [K^+], ammonium [NH_4^+], 17 carbohydrates, and 10 organic acids) by ion chromatography (Chow and Watson, 2017) and for WSOC by combustion and non-dispersive infrared detection. Citric acid and sodium chloride impregnated cellulose-fiber filters placed behind the Teflon-membrane and quartz-fiber filters, respectively, acquired NH_3 as NH_4^+ and HNO_3 as volatilized nitrate, respectively, with analysis by ion chromatography. Details on chemical analyses can be found in Chow et al. (2019).

The open face sampling manifold allows homogenous particle deposits on 47-mm filters (Watson et al., 2017). To test the uniformity of particle deposits, five individual punches were removed from the center and each quadrant of the 47-mm quartz-fiber filter disc for carbon analyses. Table S2 shows total carbon (TC = OC + EC) concentration variations of 1.7 % to 5 % across the filters for the five test burns, within the overall uncertainty of the emission estimates. Standard deviations from the five filter punches for each experiment are low with coefficients of variation of 1.7–5.0 %.

2.4 Modified combustion efficiency and fuel-based emission factors

The modified combustion efficiency (MCE) is defined as the ratio of background-subtracted CO_2 to the sum of CO_2 and CO (Ward and Radke, 1993):

$$\mathrm{MCE} = \frac{\Delta CO_2}{\Delta CO_2 + \Delta CO} \quad (1)$$

where ΔCO_2 and ΔCO are CO_2 and CO concentrations above background. MCE provides a real-time indicator of the combustion status (e.g., MCE > ~0.9 for flaming and MCE <~0.85 for smoldering).

Each burn was completed when concentrations of pollutants measured on-line (i.e., CO, NO_x, NO_y, and $PM_{2.5}$) returned to the baseline/background levels. Dilution ratios ranging from 2.7 to 5 were taken into account when calculating EFs. Fuel-based EFs are calculated based on carbon mass balance, expressed as grams of emission per kilogram of dry fuel (g kg^{-1}) (Wang et al., 2012). For gaseous and particle species *i*, the time-integrated EF_i is:

$$\mathrm{EF}_i = \mathrm{CMF}_{\mathrm{fuel}} \frac{\mathrm{C}_i}{\mathrm{C}_{\mathrm{CO_2}}\left(\frac{\mathrm{M_c}}{\mathrm{M_{CO_2}}}\right)+\mathrm{C_{CO}}\left(\frac{\mathrm{M_c}}{\mathrm{M_{CO}}}\right)+\mathrm{C_{CH_4}}\left(\frac{\mathrm{M_c}}{\mathrm{M_{CH_4}}}\right)+\sum_j \mathrm{C_{VOC}}_j\left(\frac{\mathrm{n}_j\times\mathrm{M_c}}{\mathrm{M_{VOC}}_j}\right)+\mathrm{PM_c}} \times 1000 \quad (2)$$

where CMF_{fuel} is the carbon mass fraction of the fuel in kg carbon per kg of fuel; C_i, C_{CO_2}, C_{CO}, C_{CH_4}, and C_{VOC_j} are the background-subtracted concentrations for species *i* (e.g., nitrogen or $PM_{2.5}$ species), CO_2, CO, CH_4, and VOC (C_2–C_6) species *j* in mg m^{-3} under standard conditions (temperature = 293K and pressure = 1 atm), respectively; PM_c is the total carbon concentration of $PM_{2.5}$ in mg m^{-3}; M_C, M_{CO_2}, M_{CO}, M_{CH_4}, and M_{VOC_j} are the atomic or molecular weights of carbon,

CO_2, CO, CH_4, and VOC species *j* in mg per mole, respectively; n_j is the number of carbon atom in VOC species *j*; and the factor 1000 converts kg to g. All concentrations are converted to stack concentration, i.e., species measured after dilution are adjusted by the dilution ratio. Equation 2 assumes that the carbon mass in unmeasured VOCs and other emissions not listed above is negligible compared to that in CO_2, CO, CH_4, measured VOCs (C2–C6), and $PM_{2.5}$ carbon.

2.5 Estimation of wall losses

Gas and particle wall losses can result in some underestimation of measured EFs, but it is well within the measurement uncertainties of ± 15 %. Losses can occur inside the combustion chamber, in the exhaust stack, sampling lines, and inside the OFR. Due to the low surface-to-volume ratio of the chamber (2.9 m^{-1}) and short residence time (~3 min) in this study, the gas and particle losses are expected to be low in the combustion chamber. Grosjean (1985) estimated an NH_3 loss rate of 4-17 × 10^{-4} min^{-1} in a small Teflon chamber (3.9 m^3) with a surface-to-volume ratio of 3.8 m^{-1}, resulting in < 0.5 % NH_3 wall loss. Even though the NH_3 accommodation coefficient might be higher for aluminum than Teflon (Neuman et al., 1999), the chamber wall loss in this study is expected to be < 5 % for NH_3. To reduce wall losses of sticky gases, the FTIR sampled exhaust gas from the stack without dilution, as shown in Fig. 2. Approximately 9 % NH_3 would encounter the stack wall due to turbulent diffusion (Hinds, 1999). The maximum NH_3 loss in the stack is <9 % and the maximum overall NH_3 loss is <14 %. Losses of less sticky gases would be lower.

The particle wall loss rates by McMurry and Grosjean (1985) and Wang et al. (2018) indicate <5 % particle number losses for 10 nm–2.5 μm in a similar chamber. Particle losses by turbulent diffusion in the stack are also low (<0.5 %). For a 2 m-long horizontal heated sampling line in this study (Fig. 2), particle losses by diffusion and gravitational settling are negligible (<0.1 %) for 10 nm - 1 μm particles and ~6 % for 2.5 μm particles. Earlier measurements showed that the dilution tunnel had ~100% penetration for 0.5-5 μm particles (Wang et al., 2012). Therefore, maximum particle losses in this study are estimated to be <5 % for 10 nm - 1 μm and <10 % for 2.5 μm. Past studies (Bhattarai et al., 2018;Karjalainen et al., 2016;Lambe et al., 2011) showed that particle number losses through the OFR may be ~50 % for 20 nm and <10 % for >100 nm particles, with a negligible effect on mass concentration.

3 Results and discussion

3.1 Fuel composition

Table 1 shows that peat contains 44–57 % C and 31–39 % O with the exception of the two Guizhou, China peats (20–30 % C and 21–24 % O). The carbon content (50.6 ± 2.5 % C) in Borneo, Malaysian peat is within the range of carbon fractions reported for Kalimantan and Sumatra, Indonesia peat (44–60 % C) (Christian et al., 2003;Hatch et al., 2015;Iinuma et al., 2007;May et al., 2014;Setyawati et al., 2017). The low carbon content (20–30 % C) of Guizhou peats is similar to the 28–30 % C reported for two eastern North Carolina, USA peats (Black et al., 2016).

Hydrogen contents of 2–7 % H in Table 1 are consistent with abundances found elsewhere, including: 1) ~6 % H for northern Minnesota, USA peat (Yokelson et al., 1997); 2) ~2–3 % H for the eastern North Carolina peat (Black et al., 2016); and 3) ~5–7 % H for Indonesian peats (Christian et al., 2003;Hatch et al., 2015;Iinuma et al., 2007). Sulfur (S) contents are below detection limits (<0.01 %), and nitrogen contents are 1–4 % N. Ratios of N/C are 0.02–0.08, consistent with the reported N/C ratios of: 1) 0.036 for Neustädter Moor, northern Germany (Iinuma et al., 2007); 2) 0.017–0.04 for Ireland and United Kingdom (Wilson et al., 2015); 3) 0.02–0.03 for Alberta and Ontario, Canada (Stockwell et al., 2014); 4) 0.062 for Minnesota, U.S.A. (Yokelson et al., 1997); 5) 0.022–0.03 for the eastern coast of North Carolina, U.S.A. (Black et al., 2016); and 6) 0.036–0.039 for Kalimantan and Sumatra, Indonesia (Christian et al., 2003;Hatch et al., 2015).

The sum of elements (i.e., C, H, N, S, and O) accounts for 91–98 % of total mass except for the Guizhou peats (47–56 %). As Guizhou peats appear to be a mixture of peat and soil, these samples may represent degraded peats (Miettinen et al., 2017) or contain additional minerals or high ash contents, similar to North Carolina peats (44–62 % ash, Black et al., 2016). Therefore, these peats were only used for preliminary testing of sample ignition and heating to optimize burning conditions. Overall, the six other peats in Table 1 represent biomes from different regions of the world.

3.2 Emission factors (EFs)

Table S3 summarizes the 40 peat combustion tests with the peat masses before and after each burn. The after burn residue may have contained unburned peat as well as non-combustible ash. The residues were not analyzed for carbon and nitrogen contents. A few samples were voided

due to sampling abnormalities. The following analyses are based on the 32 paired (Fresh vs Aged) samples at 25 % fuel moisture and 3 paired samples at 60 % fuel moisture. The amount of fuel consumed per test ranged from 21–48 g for all but Russian peat (14–15 g) due to limited supply.

$PM_{2.5}$ mass concentrations, in the range of 328–2277 μg/m^3, are one to two orders of magnitude higher than those commonly measured at ambient monitoring sites. Typical sample durations from ignition to completion were ~40–60 minutes, except for the Everglades (FL) peats that took longer (up to 135 minutes). Similar particle loadings (mostly within ± 20 %) were found for downstream (aged) and upstream (fresh) samples. The exception is Everglades (FL) peat, where prolonged sample durations and 7-days aging times resulted in higher downstream particle loadings with ratios of aged/fresh mass concentrations ranging 1.6–2.0.

3.2.1 Gaseous carbon emission factors

Individual and average carbonaceous gas EFs are summarized in Table S4. As shown in Fig. S4, variations by biome are found among the different peats with relative standard deviations ranging from 2–27 %. The largest EFs are found for CO_2 (EF_{CO_2}), ranging from 994–1455 g kg^{-1}, which are 1–2 orders of magnitude higher than the corresponding EF_{CO} and EF_{CH_4}. Average EF_{CO_2} varied by >30 % among biomes, ranging from 1073 ± 61 to 1400 ± 38 g kg^{-1} for the Russian and Alaskan peats, respectively.

Muraleedharan et al. (2000) reported the first laboratory-combustion EFs of 150–185 g kg^{-1} for EF_{CO_2}, 15–37 g kg^{-1} for EF_{CO}, and 6–11 g kg^{-1} for EF_{CH_4} on a wet mass basis for Brunei peat with a 51.4 % moisture content. Table 2 shows studies conducted over the past decade, with more field monitoring during the 2015 ENSO period in Indonesia. Open path (OP)-FTIR was commonly used to acquire gaseous emissions with MCEs ranging 0.77–0.86, consistent with smoldering combustion. A limited number of burns (n of 1 to 6) were conducted in laboratories using combustion chambers, whereas a larger number of in situ field-burn samples (n of 17 to 35) were acquired for southeast Asian peats (Setyawati et al., 2017;Stockwell et al., 2016;Wooster et al., 2018).

Table 2 exhibits >2-fold variations in EF_{CO_2} among studies. The highest EF_{CO_2} with the lowest variability was found for tropical peats (ranges 1331–1831 g kg^{-1} for smoldering). Average EF_{CO_2} (1331 ± 78 g kg^{-1}) for Malaysian peat (n=6) from this study is ~16 % and ~18 % lower than the 1579 ± 58 and 1615 ± 184 g kg^{-1} for Peninsula, Malaysia (Smith et al., 2018) and average

boreal/temperate peats (Hu et al., 2018), respectively. Malaysian peat EF_{CO_2} measured in this study is 20 % lower than the 1681 ± 96 g kg^{-1}, averaged from seven studies of Kalimantan and Sumatra, Indonesia peats (Christian et al., 2003;Huijnen et al., 2016;Nara et al., 2017;Stockwell et al., 2014).

Overall average EF_{CO_2} (1269 ± 139 g kg^{-1}, n=32) from this study (Table S4) are ~19–25 % lower than the 1563 ± 65 g kg^{-1} for peatland fires used in atmospheric models (Akagi et al., 2011); 1550 ± 130 g kg^{-1} in a recent review (Andreae, 2019); and 1703 g kg^{-1} (Christian et al., 2003) adopted by the 2014 Intergovernmental Panel on Climate Change (IPCC) for organic soil fire inventories (IPCC, 2014). EFs derived from this study cover four biomes which may improve global emission estimates.

Average EF_{CO} is typically ~12–15 % of EF_{CO_2} in the range of 157–171 g kg^{-1} for all but the two Florida peats with 394 ± 46 g kg^{-1} (MCE = 0.65 ± 0.04) and 93 ± 21 g kg^{-1} (MCE = 0.90 ± 0.03) for the Putnam and Everglades peats, respectively (Table S4 and Table 2). This is consistent with a higher EF_{CO} under lower MCEs reported by Setyawati et al. (2017) –a 45-fold increase from 3.1 ± 7.2 g kg^{-1} for flaming (MCE = 0.998 ± 0.005) to 138 ± 72 g kg^{-1} for smoldering (MCE = 0.894 ± 0.055) combustion.

Average EF_{CO} of 157–161 g kg^{-1} for boreal and temperate peats are ~10 % lower than the 179 ± 61 g kg^{-1} from Hu et al. (2018). The overall average EF_{CO} of 175 ± 92 g kg^{-1} from this study is ~4 % lower than the 182 ± 60 g kg^{-1} in Akagi et al. (2011), ~30 % lower than the 250 ± 23 g kg^{-1} in Andreae (2019), and ~15 % lower than the 207–210 g kg^{-1} used in IPCC (2014).

Average EF_{CH_4} is ~0.3–0.9 % of EF_{CO_2}, lowest for cold climates with 3.2–6.9 g kg^{-1} for the boreal and temperate peats and 6.7–10.4 g kg^{-1} for the subtropical and tropical peats (Table S4). Table 2 shows that EF_{CH_4} for Malaysian and Indonesian peats exceed ~10 g kg^{-1} in five of the eight past studies. These EFs are more in line with the 11.8 ± 7.8 g kg^{-1} in Akagi et al. (2011), 9.3 ± 1.5 g kg^{-1} in Andreae (2019), and 9–21 g kg^{-1} in IPCC (2014), but are higher than the average (6.6 ± 2.4 g kg^{-1}) found in this study.

Emission factors depends on both fuel composition and combustion conditions. Figure S5a shows that total measured gas and particle carbon increases with fuel carbon content for the six types of peat. EF_{CO_2} increases with fuel carbon content (Fig. S5b) except for the Putnam (FL) peat, which has the highest fuel carbon (56.6 %) but low EF_{CO_2}. It has high EF_{CO} and EF_{TC} (Figs. S5c-

d), consistent with its low MCE (0.65 ± 0.04). EF_{CO} and EF_{TC} do not show a clear trend with fuel carbon content; however, EF_{CH_4} increases with fuel carbon (Fig. S5e) but decreases with fuel oxygen content (Fig. S5f).

3.2.2 Gaseous nitrogen emission factors

Individual and average gaseous nitrogen species EFs are summarized in Table S5. EF_{NO} and EF_{NO_2} (Fig. S6b) are low in the range of 0.2–2.1 g kg^{-1}. For fresh emissions, most of the NO_x (NO + NO_2) is present as NO. After the OFR, NO decreased while NO_2 increased, as shown in Fig. S7. A low correlation coefficient (r = 0.67) between the downstream and upstream EF_{NO_x} suggests the changes of NO/NO_2 ratios between the fresh and aged emissions as well as variabilities among tests.

Table 3 shows that most studies do not report EF_{NO} or EF_{NO_2}, partially due to the low concentrations and large variabilities under atmospheric aging. Stockwell et al. (2014;2016) reported 0.31–1.85 g kg^{-1} EF_{NO} and 2.31–2.36 g kg^{-1} EF_{NO_2} for Indonesia peats. These levels are much higher than the EF_{NO_x} (as NO_2) of 0.75 ± 0.10 g kg^{-1} for Malaysian peat in this study.

Emissions for reactive nitrogen, EF_{NO_y} (as NO_2), ranged 0.61–6.3 g kg^{-1} with an average of 2.4 ± 1.4 g kg^{-1} (Table S5). EF_{NO_y} >2.5 g kg^{-1} are found for the two Florida peats (Fig S6c) with an average of 4.3 ± 1.1 g kg^{-1} for Everglades, which reports the highest nitrogen content (3.93 ± 0.08 %) among peats (Table 1). Figure S5g shows that EF_{NO} increases with fuel nitrogen content, while EF_{NO2} is not dependent on fuel nitrogen content (Fig. S5h). Because EF_{NO} is higher than EF_{NO2}, EF_{NOx} and EF_{NOy} increase with fuel nitrogen content (not shown). Figure S8 shows that ~74 % of the NO_y is NO_x with high correlation coefficient (r = 0.93). Nitrogen oxides are typically converted to other oxidized nitrogen species within 24 hours after emission (Prenni et al., 2014;Seinfeld and Pandis, 1998). The ratio of NO_x/NO_y has been used to infer photochemical aging (Kleinman et al., 2003;Kleinman et al., 2007;Olszyna et al., 1994;Parrish et al., 1992). The high NO_x/NO_y ratios suggest that NO_x had not converted to other reactive nitrogen species in the diluted peat plume.

Nitrous oxide (N_2O), an inert form of oxide from nitrogen with an atmospheric lifetime of ~110 years, commonly emitted from fossil fuel, solid waste fertilizers, and biomass combustion, is a greenhouse gas defined by U.S. EPA (2016). Table S5 shows that EF_{N_2O} are similar to EF_{NO_y}

except for Everglades (FL) peat with low EF_{N_2O} (1.5 ± 0.3 g kg^{-1}), in the range of 1.1–4.4 g kg^{-1} and average of 2.0 ± 0.7 g kg^{-1}. The highest average EF_{N_2O} (3.6 ± 0.6 g kg^{-1}) is found for Putnam (FL) peat (Fig. S6c).

Hydrogen cyanide (HCN), a known emission from biomass burning (Li et al., 2000;Stockwell et al., 2014), exhibits >7-fold differences (1.8–14 g kg^{-1}) in EF_{HCN} (Table S5). The average EF_{HCN} (11.5 ± 2.3 g kg^{-1}) for Putnam (FL) peat is 2- to 5-fold higher than for the other biomes (Fig. S6a). Table 3 shows large EF_{HCN} variations among studies, from 0.73 ± 0.50 g kg^{-1} (Ireland, Wilson et al., 2015) to 5.75 ± 1.60 g kg^{-1} (Indonesia, Stockwell et al., 2016). More consistent EF_{HCN} are found for tropical peats in the range of 3–6 g kg^{-1}. Average EF_{HCN} in this study, 4.7 ± 3.1 g kg^{-1}, are in-line with the 5.0 ± 4.9 and 4.4 ± 1.2 g kg^{-1} reported by Akagi et al. (2011) and Andreae (2019).

EF_{NH_3} (0.4–8.3 g kg^{-1}) are of the same magnitude as EF_{HCN} (Fig. S6a) and independent of fuel nitrogen content (Fig. S5i) except for the Everglades (FL) peat (9–18 g kg^{-1}) which has the highest fuel nitrogen content. Total reduced nitrogen emissions, EF_{NH_3} + EF_{HCN}, for the two Florida peats (12–25 g kg^{-1}) are ~2- to 3-fold higher than those for other regions. Table 3 also shows high variabilities in EF_{NH_3} among studies (1–11 g kg^{-1}). The overall average of 5.6 ± 4.8 g kg^{-1} in this study is consistent with the 4.2 ± 3.2 g kg^{-1} in Andreae (2019), but ~50 % of the 10.8 ± 12.4 g kg^{-1} in Akagi et al. (2011). The high standard deviations associated with these averages signify large variabilities among experiments.

Figure S9a shows some difference in EF_{NH_3} determined by FTIR and the impregnated filter, especially at high concentrations. The regression slope shows that EF_{NH_3} by the FTIR was ~22 % lower than that of filters with a correlation coefficient of 0.76. Variable baselines in the FTIR measurements along with some nitrogen content in the diluted air and breath NH_3 (Hibbard and Killard, 2011) in the testing laboratory may have contributed to these variations. The impregnated filter collects all of the NH_3 over the sampling period, including amounts that are below the FTIR detection limits, so it is probably better representing the time-integrated EF_{NH_3}. Reduction of EF_{NH_3} is most apparent after atmospheric aging in Fig. S9b (slope of 0.11), with 2–14 g kg^{-1} in fresh emissions and reduced to ~0.5–3 g kg^{-1} after aging.

3.2.3 $PM_{2.5}$ mass and carbon emission factors

Continuous $PM_{2.5}$ from the DustTrak with the factory calibration factor yielded $PM_{2.5}$ EFs 3- to 5 times higher than of those derived from gravimetric analyses, higher than the 2-fold mass differences by Wooster et al. (2018). This discrepancy is well known as the factory calibration uses Arizona road dust with a size distribution that is much coarser than that of biomass burning. Therefore, $EF_{PM_{2.5}}$ is calculated from the filter samples. Chow et al. (2019) present the species abundances in $PM_{2.5}$ mass for this study based on the average fresh and aged profiles, separated by 2- and 7-day photochemical aging times simulated with the OFR (Aerodyne, 2019). The same approach is used in Table S6 to compare fresh and aged particle EFs. Comparisons between combined fresh vs. aged EFs for $PM_{2.5}$ mass, carbon (OC, EC, and TC), and levoglucosan for individual tests are shown in Table S7.

Figure S10 shows that $EF_{PM_{2.5}}$ varies >4-fold (14–61 g kg^{-1}) for different peats without large differences between fresh and aged emissions. EF_{OC} varied from 9–44 g kg^{-1} while EF_{EC} (0.00–2.2 g kg^{-1}) were low (Table S7). The majority of $EF_{PM_{2.5}}$ consist of EF_{OC}, with average $EF_{OC}/EF_{PM_{2.5}}$ ratios of 52–98 % by peat type in fresh emissions, followed by ~14–23 % reductions after aging, with the exception of Putnam (FL) peats (remained at 69–70 %).

Reductions of EF_{OC} after ~7 days of photochemical aging are most apparent (~7–9 g kg^{-1}) for the boreal peats, with the largest degradation for low temperature OC1 (evolved at 140°C during carbon analysis), indicating losses of high vapor pressure SVOCs upon aging (Table S6). The two Florida peats exhibit an initial EF_{OC} decrease of ~2 g kg^{-1} after 2-days aging, but with an increase of 1.8–4.0 g kg^{-1} after 7 days. However, these changes are less than the standard deviations associated with the averages.

EF_{WSOC} varies by 5-fold (3–16 g kg^{-1}) with over a ~50 % increase for the Putnam (FL) and Malaysian peats after 7 days. Average EF_{WSOC} by peat type accounts for ~16–36 % and ~20–62 % of fresh $EF_{PM_{2.5}}$ and EF_{OC}, respectively. From 2- to 7-day aging, Fig. S11 shows reduced correlation coefficients (r from 0.86 to 0.76 for $PM_{2.5}$, from 0.88 to 0.84 for OC, and 0.94 to 0.68 for WSOC).

As WSOC is part of the OC, the WSOC/OC ratio can be used to illustrate atmospheric aging. Figure S12 shows that WSOC/OC ratios increased by 6–16 % after aging. This is attributed to a combination of oxygenation of the aged organic emissions and the reduction of EF_{OC} (Table

443 S7). The increase in WSOC/OC ratios may also be due to photochemical transformation of primary
444 OC to WSOC and/or formation of water-soluble SOA during atmospheric aging (Agarwal et al.,
445 2010;Aggarwal and Kawamura, 2009).

446 Table 4 compares filter-based PM mass and carbon from different studies. Since different
447 carbon protocols yield different fractions of OC and EC (Watson et al 2005), the analytical
448 protocols are listed. Most studies follow either IMPROVE_A TOR (Chow et al., 2007) or NIOSH
449 thermal/optical transmittance (TOT) protocols (NIOSH, 1999). As the transmittance pyrolysis
450 correction (i.e., TOT) accounts for charred OC both on the filter surface and organic vapor within
451 the filter substrate, lower EF_{EC} are expected as compared to TOR (Chow et al., 2004). To remove
452 the OC and EC split uncertainty, TC to PM mass ratios are listed for comparison. Two studies
453 reported black carbon (BC) from a micro-aethalometer (Wooster et al., 2018) or a single particle
454 soot photometer (SP2; May et al., 2014). As BC levels are very low, not much differences can be
455 distinguished between BC and EC .

456 Most studies report $EF_{PM_{2.5}}$ with a few exceptions for $EF_{PM_{10}}$ (Iinuma et al., 2007;Kuwata
457 et al., 2018) and EF_{PM_1} (May et al., 2014). As most of the PM_{10} is in the $PM_{2.5}$ fraction for biomass
458 combustion, particle size fractions have a minor effect on PM EFs (Geron and Hays, 2013;Hu et
459 al., 2018).

460 Table 4 shows that the majority of $EF_{PM_{2.5}}$ lies in the range of ~20–50 g kg^{-1} with the
461 exception of very low $EF_{PM_{2.5}}$ of 4–8 and 6–7 g kg^{-1} reported by Bhattarai et al. (2018) and Black
462 et al. (2016). These are probably due to low filter mass loadings and limited testing (n of 1 to 3),
463 which may result in large uncertainties in gravimetric mass.

464 Despite different carbon analysis methods, most EF_{OC} lies in the range of ~5–30 g kg^{-1} with
465 the exception of EF_{OC} (37 g kg^{-1}) for Putnam (FL) and EF_{OA} (organic aerosol, 34.5 g kg^{-1}) for
466 Indonesian peat measured by a time-of-flight/mass spectrometer (May et al., 2014). Most studies
467 show that EF_{TC} accounts for ~60–85 % of the $EF_{PM_{2.5}}$, with low EF_{EC} (0.02–1.3 g kg^{-1}).

468 EF_{WSOC} of 6–7 and 4–6 g kg^{-1} for the Alaskan and Malaysian peats from this study are
469 consistent with the 6.7 and 3.1 g kg^{-1} from German and Indonesian peats in Iinuma et al. (2007),
470 respectively. $EF_{Levoglucosan}$ exhibits >2 orders of magnitude variabilities among the biomes with
471 0.24–16 g kg^{-1} and 0.24–9.6 g kg^{-1} in fresh and aged emissions, respectively.

Past studies show that the extent of levoglucosan degradation depends on OH exposure in the OFR, organic aerosol composition, and vapor wall losses (e.g., Bertrand et al., 2018a;2018b;Hennigan et al., 2010;Hoffmann et al., 2010;Lai et al., 2014;May et al., 2012;Pratap et al., 2019). Potential chemical pathways for the formation of organic species in biomass combustion emissions were proposed by Gao et al. (2003) that suggested the fragmentaion of levoglucosan to C3–C5 diacids, followed by oxalic acid, acetic acid, and formic acid. This is consistent with the increases in $EF_{organic\ acids}$ after atmospheric aging, as shown in Table S6. However, detailed chemical mechanisms need to be further investigated.

The highest $EF_{Levoglucosan}$ is found for the fresh Russian peats (15.8 ± 2.9 g kg^{-1}), and this is diminished by 45 % after 7-day aging (8.8 ± 2.1 g kg^{-1}). Few studies report $EF_{Levoglucosan}$ and results are highly variable. The $EF_{Levoglucosan}$ of 0.57 g kg^{-1} in $PM_{2.5}$ (converted from 46 mg/g OC) by Jayarathne et al. (2018) is ~23 % of the 2.5 g kg^{-1} by Iinuma et al. (2007), both for Indonesia peats. The $EF_{Levoglucosan}$ of 0.5–1.0 g kg^{-1} from fresh Malaysian peat in this study is comparable to 0.57 g kg^{-1} by Jayarathne et al. (2018). The 4.6 g kg^{-1} of $EF_{Levoglucosan}$ for the northern German peat (Iinuma et al., 2007) is higher than the 1.2–4.7 g kg^{-1} found for the average Siberian and Alaskan peats in this study.

EFs for ionic nitrogen species are low (<0.1 g kg^{-1}) in fresh emissions. Both $EF_{NH_4^+}$ and $EF_{NO_3^-}$ increase with 7-day aging – >0.5 g kg^{-1} $EF_{NH_4^+}$ for all peat and >1 g kg^{-1} $EF_{NO_3^-}$ for all but Russian (0.79 ± 0.08 g kg^{-1}) and Putnam (FL) peats (0.66 ± 0.08 g kg^{-1}), consistent with the formation of secondary inorganic aerosol.

3.3 Effect of fuel moisture content on emission factors

Only a few studies examine the effects of fuel moisture on peat emissions with inconsistent results. An early study by McMahon et al. (1980) reported high emissions for total suspended particle (TSP, ~<30–60 μm) of 30 ± 20 g kg^{-1} for dry (<11 % moisture) as compared to 4.1 ± 3.8 g kg^{-1} (after the first 24 hours) for wet (53–97 % moisture) organic soil. Rein et al. (2009) found higher CO_2 (but not CO) yields while increasing fuel moisture to 600 % for tests of boreal Scotland peats in a cone calorimeter which continuously supplies heat to the fuel. Smoldering combustion is possible with high *in situ* fuel-moisture contents when surrounding peat provides insulation and heat from combustion is available for drying just before the advancing front, but such samples will not burn in the laboratory. Watts (2013) sustained lab-based peat smoldering from a cypress swamp (FL) at ~250 % moisture content, which appears to be a maximum.

503 Table 2 shows that increasing moisture content from ~25 % to ~60 % for the three Putnam
504 (FL) peats resulted in a 11 % increase in EF_{CO_2} but reductions of 20 % EF_{CO} and 12 % EF_{CH_4}. No
505 consistent variabilities are found for nitrogen species (Table 3), with negligible changes in EF_{NH_3}
506 and EF_{HCN}; 13–30 % reduction in EF_{NO}, EF_{NO_x}, and EF_{NOy}, as well as 45 % increase in EF_{NO_2} and
507 9 % increase in EF_{N_2O}. On the other hand, a reduction of ~30 % $EF_{PM_{2.5}}$ is found (Table 4) as fuel
508 moisture increased from 25 % to 60 %. Higher fuel moisture contents typically result in less
509 efficient burning conditions, thereby increasing CO and reducing MCE (Chen et al., 2010).
510 However, an opposite trend is found with EF_{CO} reduced from 394 ± 46 to 315 ± 10 g kg^{-1} and
511 MCEs increased from 0.65 ± 0.04 to 0.72 ± 0.01. It is hypothesized that at higher fuel moisture
512 contents, combustion residence time is slowed enough so that radiant heat transfer from ignited
513 particles to uncombusted areas of peat can be greater, thus increasing the combustion efficiency.
514 Overall, the EFs for ~60 % moisture contents are comparable to EFs for the six other peats with
515 ~25 % moisture content.

516 Increased (~25 to 60 %) fuel moisture yields a ~20 % reduction in fresh EF_{OC}, much lower
517 than the 35–43 % reduction (~25 to 50 % moisture) reported by Chakrabarty et al. (2016) for the
518 Siberian and Alaskan peats. By increasing fuel moisture, Chakrabarty et al (2016) also reported an
519 increase in EF_{CO_2} by 20 % but a ~75 % reduction and 35 % increase in EF_{CO} for Siberian and
520 Alaskan peats, respectively, based on a single sample.

521 **3.4 Distribution of carbon and nitrogen species**

522 Figure 3 shows the distribution of carbonaceous species. Because the EFs are calculated
523 based on the carbon mass balance method (Eq. (2)), the total emitted carbon is assumed to be the
524 same as total consumed carbon. The majority (>90 %) of total emitted carbon are present in the
525 gas phase with 54–75 % CO_2, followed by 8–30 % CO. On average, emitted carbon includes 69.8
526 ± 7.5 % CO_2; 14.8 ± 6.5 % CO; 1.0 ± 0.3 % CH_4; 9.4 ± 2.4 % volatile carbon compounds; and 4.8
527 ± 1.3 % $PM_{2.5}$ TC. The highest (30 ± 4 %) and lowest (8.4 ± 1.9 %) CO abundances for the Putnam
528 (FL) and Everglades (FL) peats are consistent with the lowest and highest average MCEs of 0.65
529 and 0.90, respectively.

530 The nitrogen budget in Fig. 4 accounts for 24–52 % of nitrogen in the consumed fuel. Since
531 burn temperatures are below those at which NO_x forms from oxygen reactions with N_2 in the air,
532 most of the nitrogen in emissions derives from the nitrogen content of the fuels. Kuhlbusch et al.

(1991) found N_2 emissions constituted an average of 31 ± 20 % of nitrogen in consumed grass, hay, pine needle, clover, and wood fuels. Since N_2 measurements require combustion in N_2-free atmosphere (e.g., a He-O_2 mixture), N_2 was not quantified here, but it was probably emitted in similar quantities. Isocyanic acid (HNCO) is another important nitrogen-containing compound found in biomass burning emissions (Roberts et al., 2011). Koss et al. (2018) report a 0.16 g/kg nitrogen-equivalent EF (0.5 g/kg for HNCO) for a peat sample, comparable to EFs for several of the measured nitrogen compounds summarized in Table 3. Other nitrogen-containing gases reported by Koss et al. (2018) with EFs >0.1 g/kg include acetonitrile (CH_3CN), acetamide (CH_3CONH_2), benzonitrile (C_6H_5CN), and pyridine + pentadienenitriles (C_5H_5N), which could account for part of the unmeasured nitrogen in emissions. Neff et al. (2002) found that organic nitrogen formed from photochemical reactions of hydrocarbon with NO_x plays an important role in the global nitrogen cycle. Approximately 30 ± 16 % of Neff et al.'s total nitrogen was from organic nitrogen, similar to the 25 % of total nitrogen deposition flux reported by Jickells et al. (2013). Alkaloids, dissolved organic nitrogen, along with nitroaromatic compounds have been reported (e.g., Benitez et al., 2009;Kopacek and Posch, 2011;Koppmann et al., 2005;Kuhlbusch et al., 1991;Laskin et al., 2009;Stockwell et al., 2015).

The majority (>99 %) of the measured nitrogen in emissions is in the gas phase. On average, 16.7 % of the fuel nitrogen was emitted as NH_3 and 9.5 % was emitted as HCN. N_2O and NO_y constituted 5.7 % and 2.9 % of nitrogen in the consumed fuel. NH_3 emissions accounted for 26–28 % of consumed nitrogen for Everglades (FL) and Malaysian peats while HCN emissions dominated fuel nitrogen(13–17 %) for the Putnam (FL) and Malaysian peats. The fraction of N_2O emissions in Malaysian peat nitrogen (10.3 ± 1.1 %) was more than twice the fractions found for the other regions with reactive nitrogen (NO_y) only accounting for 2–4 % of the fuel nitrogen. The sum of NH_3 and HCN nitrogen ranged 35–39 % of consumed nitrogen for the Malaysian and Everglades (FL) peats, which is about three times the fraction for Russian peat.

Lobert et al. (1990) point out the importance of nitrogen-containing gases in biomass burning for the atmospheric nitrogen balance. On average, the emitted nitrogen includes 17 ± 10 % NH_3, 9.5 ± 3.8 % HCN, 5.7 ± 2.5 % N_2O, 2.8 ± 1.0 % NO_y (including NO_x), and 0.14 ± 0.18 % of PM nitrogen (sum of NO_2^-, NO_3^-, and NH_4^+). The average nitrogen budget accounts for 35 ± 11 % of the total consumed nitrogen, consistent with past studies showing that ~one- to two-thirds of the fuel nitrogen is accounted for during biomass combustion.

4 Summary and conclusions

This paper reports fuel composition and emission factors (EFs) from laboratory chamber combustion of six types of peat fuels representing boreal (Russia and Siberia), temperate (northern Alaska, USA), subtropical (northern and southern Florida, USA), and tropical (Borneo, Malaysia) climate regions. Dried peat fuel contains 44–57 % carbon (C), 31–39 % oxygen (O), 5–6 % hydrogen (H), 1–4 % nitrogen (N), and <0.01 % Sulfur (S). The nitrogen to carbon ratios are low, in the range of 0.02–0.08, consistent with peat compositions reported in other studies.

Thirty-two tests with 25 % fuel moisture were reported with predominant smoldering combustion conditions (MCE = 0.82 ± 0.08). Average fuel-based EFs for CO_2 (EF_{CO_2}) are highest (1400 ± 38 g kg^{-1}) and lowest (1073 ± 63 g kg^{-1}) for the Alaskan and Russian peats, respectively. EF_{CO} and EF_{CH_4} are ~12–15 % and ~0.3–0.9 % of EF_{CO_2} in the range of ~157–171 g kg-1 and 3–10 g kg^{-1}, respectively. The exception is the two Florida peats, reporting the highest (394 ± 46 g kg^{-1}) and lowest (93 ± 21 g kg^{-1}) EF_{CO} for Putnam and Everglades, respectively.

Filter-based $EF_{PM_{2.5}}$ varied by >4-fold (14–61 g kg^{-1}) without appreciable changes between fresh and aged emissions. The majority of $EF_{PM_{2.5}}$ consists of EF_{OC}, with average $EF_{OC}/EF_{PM_{2.5}}$ ratios by peat type in the range of 52–98 % in fresh emissions, followed by ~14–23 % reduction after aging with the exception of Putnam (FL) peats (retained at 69–70 %). Reduction of EF_{OC} (~7–9 g kg^{-1}) are most apparent for boreal peats with the largest decrease in low temperature OC1 (evolved at 140°C), suggesting the loss of high vapor pressure semi-volatile organic compounds during aging. EFs for water-soluble OC (EF_{WSOC}) accounts for ~20–62 % of EF_{OC} with ~6–16 % increase in EF_{WSOC}/EF_{OC} ratios after aging. The highest $EF_{Levoglucosan}$ is found for Russian peat (15.8 ± 2.9 g kg^{-1}) with a 45 % degradation after aging.

The majority (>90 %) of the total emitted carbon is in the gas phases with 54–75 % CO_2, followed by 8–30 % CO. Nitrogen budget only explains 24–52 % of the consumed nitrogen with an average of 35 ± 11 %, consistent with past studies that ~one- to two-thirds of the total nitrogen are lost upon biomass combustion. The majority (>99 %) of the total emitted nitrogen is in the gas phase, dominated by the two reduced nitrogen species with 16.7 % for NH_3 and 9.5 % for HCN. N_2O and NO_y are detectable at 5.7 % and 2.9 % abundance. EFs from this study can be used to refine current emission inventories.

5 Author contributions

JGW, JCC, JC, L-WAC, and XW jointly designed the study, performed the data analyses, and prepared the manuscript. QW, JT, and SSHH carried out the peat combustion experiments. SG conducted emission factor calculations. ACW acquired peat fuels and provided technical advice on peat fuel process.

6 Competing interests

The authors declare that there are no conflicts of interest.

7 Acknowledgements

This research was primarily supported by the National Science Foundation (NSF, AGS-1464501 and CHE-1214163) as well as internal funding from both the Desert Research Institute, Reno, NV, USA, and Institute of Earth Environment, Chinese Academy of Sciences, Xian, China. The Caohai and Gaopo peat samples were provided by Dr. Pinhua Xia of Guizhou Normal University, Guizhou, China and Dr. Chunmao Zhu of the Japan Agency for Marine-Earth Science and Technology, Yokosuka, Japan.

8 References

Aerodyne: Potential Aerosol Mass (PAM) oxidation flow reactor, Aerodyne Research Inc., Billerica, MA, 2019. http://www.aerodyne.com/sites/default/files/u17/PAM%20Potential%20Aerosol%20Mass%20Reactor.pdf

Agarwal, S., Aggarwal, S. G., Okuzawa, K., and Kawamura, K.: Size distributions of dicarboxylic acids, ketoacids, alpha-dicarbonyls, sugars, WSOC, OC, EC and inorganic ions in atmospheric particles over Northern Japan: implication for long-range transport of Siberian biomass burning and East Asian polluted aerosols, Atmos. Chem. Phys, 10, 5839-5858, 2010.

Aggarwal, S. G., and Kawamura, K.: Carbonaceous and inorganic composition in long-range transported aerosols over northern Japan: Implication for aging of water-soluble organic fraction, Atmos. Environ., 43, 2532-2540, 2009.

Akagi, S. K., Yokelson, R. J., Wiedinmyer, C., Alvarado, M. J., Reid, J. S., Karl, T., Crounse, J. D., and Wennberg, P. O.: Emission factors for open and domestic biomass burning for use in atmospheric models, Atmos. Chem. Phys, 11, 4039-4072, 2011.

Allen, C., Carrico, C. M., Gomez, S. L., Andersen, P. C., Turnipseed, A. A., Williford, C., Birks, J. W., Salisbury, D., Carrion, R., Gates, D., Macias, F., Rahn, T., Aiken, A. C., and Dubey, M. K.: NOx instrument intercomparison for laboratory biomass burning source studies and urban ambient measurements in Albuquerque, New Mexico, J. Air Waste Manage. Assoc., 68, 1175-1189, 10.1080/10962247.2018.1487347, 2018.

Alvarado, M. J., Logan, J. A., Mao, J., Apel, E., Riemer, D., Blake, D., Cohen, R. C., Min, K. E., Perring, A. E., Browne, E. C., Wooldridge, P. J., Diskin, G. S., Sachse, G. W., Fuelberg, H., Sessions, W. R., Harrigan, D. L., Huey, G., Liao, J., Case-Hanks, A., Jimenez, J. L., Cubison, M. J., Vay, S. A., Weinheimer, A. J., Knapp, D. J., Montzka, D. D., Flocke, F. M., Pollack, I. B., Wennberg, P. O., Kurten, A., Crounse, J., St Clair, J. M., Wisthaler, A., Mikoviny, T., Yantosca, R. M., Carouge, C. C., and Le Sager, P.: Nitrogen oxides and PAN in plumes from boreal fires during ARCTAS-B and their impact on ozone: an integrated analysis of aircraft and satellite observations, Atmos. Chem. Phys, 10, 9739-9760, 2010.

Andreae, M. O.: Emission of trace gases and aerosols from biomass burning- An updated assessment, Atmospheric Chemistry and Physics Discussion, 1-27, 10.5194/acp-2019-303, 2019.

Ballenthin, J. O., Thorn, W. F., Miller, T. M., Viggiano, A. A., Hunton, D. E., Koike, M., Kondo, Y., Takegawa, N., Irie, H., and Ikeda, H.: In situ HNO_3 to NO_y instrument comparison during SOLVE, Journal of Geophysical Research, 108, ACH 7-1-ACH 7-11, 10.1029/2002JD002136, 2003.

Behera, S. N., Betha, R., Huang, X., and Balasubramanian, R.: Characterization and estimation of human airway deposition of size-resolved particulate-bound trace elements during a recent haze episode in Southeast Asia, Environmental Science and Pollution Research, 10.1007/s11356-014-3645-6, 2014.

Benitez, J. M. G., Cape, J. N., Heal, M. R., van Dijk, N., and Diez, A. V.: Atmospheric nitrogen deposition in south-east Scotland: Quantification of the organic nitrogen fraction in wet, dry and bulk deposition, Atmos. Environ., 43, 4087-4094, 2009.

Bertrand, A., Stefenelli, G., Jen, C. N., Pieber, S. M., Bruns, E. A., Ni, H. Y., Temime-Roussel, B., Slowik, J. G., Goldstein, A. H., El Haddad, I., Baltensperger, U., Prevot, A. S. H., Wortham, H., and Marchand, N.: Evolution of the chemical fingerprint of biomass burning organic aerosol during aging, Atmos. Chem. Phys, 18, 7607-7624, 10.5194/acp-18-7607-2018, 2018a.

Bertrand, A., Stefenelli, G., Pieber, S. M., Bruns, E. A., Temime-Roussel, B., Slowik, J. G., Wortham, H., Prevot, A. S. H., El Haddad, I., and Marchand, N.: Influence of the vapor wall loss on the degradation rate constants in chamber experiments of levoglucosan and other biomass burning markers, Atmos. Chem. Phys, 18, 10915-10930, 10.5194/acp-18-10915-2018, 2018b.

649 Betha, R., Pradani, M., Lestari, P., Joshi, U. M., Reid, J. S., and Balasubramanian, R.: Chemical speciation of trace
650 metals emitted from indonesian peat fires for health risk assessment, Atmospheric Research, 122, 571-578, 2013.

651 Bhattarai, C., Samburova, V., Sengupta, D., Iaukea-Lum, M., Watts, A. C., Moosmuller, H., and Khlystov, A. Y.:
652 Physical and chemical characterization of aerosol in fresh and aged emissions from open combustion of biomass
653 fuels, Aerosol Sci. Technol., 52, 1266-1282, 10.1080/02786826.2018.1498585, 2018.

654 Bin Abas, M. R., Rahman, N. A., Omar, N. Y. M. J., Maah, M. J., Abu Samah, A., Oros, D. R., Otto, A., and
655 Simoneit, B. R. T.: Organic composition of aerosol particulate matter during a haze episode in Kuala Lumpur,
656 Malaysia, Atmos. Environ., 38, 4223-4241, 2004.

657 Black, R. R., Aurell, J., Holder, A., George, I. J., Gullett, B. K., Hays, M. D., Geron, C. D., and Tabor, D.:
658 Characterization of gas and particle emissions from laboratory burns of peat, Atmos. Environ., 132, 49-57,
659 10.1016/j.atmosenv.2016.02.024, 2016.

660 Cao, J. J., Wang, Q. Y., Tan, J., Zhang, Y. G., Wang, W. J., Zhong, B. L., Ho, S. S. H., Chen, L.-W. A., Wang, X.
661 L., Watson, J. G., and Chow, J. C.: Evaluation of the oxidation flow reactor for particulate matter emission limit
662 certification, Atmos. Environ., submitted, 2019.

663 Chakrabarty, R. K., Gyawali, M., Yatavelli, R. L. N., Pandey, A., Watts, A. C., Knue, J., Chen, L. W. A., Pattison,
664 R. R., Tsibart, A., Samburova, V., and Moosmuller, H.: Brown carbon aerosols from burning of boreal peatlands:
665 microphysical properties, emission factors, and implications for direct radiative forcing, Atmos. Chem. Phys, 16,
666 3033-3040, 10.5194/acp-16-3033-2016, 2016.

667 Chen, Y., Randerson, J. T., van der Werf, G. R., Morton, D. C., Mu, M., and Kasibhatla, P. S.: Nitrogen deposition
668 in tropical forests from savanna and deforestation fires, Global Change Biology, 16, 2024-2038, 2010.

669 Cheng, Y. H., Shiu, B. T., Lin, M. H., and Yan, J. W.: Levels of black carbon and their relationship with particle
670 number levels-observation at an urban roadside in Taipei City
671 CHENG2013A, Environmental Science and Pollution Research, 20, 1537-1545, 2013.

672 Chow, J. C., Watson, J. G., Chen, L.-W. A., Chang, M.-C. O., Robinson, N. F., Trimble, D. L., and Kohl, S. D.: The
673 IMPROVE_A temperature protocol for thermal/optical carbon analysis: Maintaining consistency with a long-term
674 database, J. Air Waste Manage. Assoc., 57, 1014-1023, 2007.

675 Chow, J. C., Wang, X. L., Sumlin, B. J., Gronstal, S. B., Chen, L.-W. A., Trimble, D. L., Kohl, S. D., Mayorga, S.
676 R., Riggio, G. M., Hurbain, P. R., Johnson, M., Zimmermann, R., and Watson, J. G.: Optical calibration and
677 equivalence of a multiwavelength thermal/optical carbon analyzer, Aerosol Air Qual. Res., 15, 1145-1159,
678 doi:10.4209/aaqr.2015.02.0106, 2015.

679 Chow, J. C., and Watson, J. G.: Enhanced ion chromatographic speciation of water-soluble $PM_{2.5}$ to improve
680 aerosol source apportionment, Aerosol Science and Engineering, 1, 7-24, doi:10.1007/s41810-017-0002-4, 2017.

681 Chow, J. C., Cao, J., Chen, L.-W. A., Wang, X. L., Wang, Q. Y., Tian, J., Ho, S. S. H., Carlson, T. N., Kohl, S. D.,
682 and Watson, J. G.: Evaluating changes in $PM_{2.5}$ peat combustion source profiles with atmospheric aging in an
683 oxidation flow reactor, Atmos. Meas. Tech., online, 2019.

684 Christian, T. J., Kleiss, B., Yokelson, R. J., Holzinger, R., Crutzen, P. J., Hao, W. M., Saharjo, B. H., and Ward, D.
685 E.: Comprehensive laboratory measurements of biomass-burning emissions: 1. Emissions from Indonesian, African,
686 and other fuels, Journal of Geophysical Research, 108, 2003.

687 Crutzen, P. J., and Andreae, M. O.: Biomass burning in the tropics: Impact on atmospheric chemistry and
688 biogeochemical cycles, Science, 250, 1669-1678, 1990.

689 Cubison, M. J., Ortega, A. M., Hayes, P. L., Farmer, D. K., Day, D., Lechner, M. J., Brune, W. H., Apel, E., Diskin,
690 G. S., Fisher, J. A., Fuelberg, H. E., Hecobian, A., Knapp, D. J., Mikoviny, T., Riemer, D., Sachse, G. W., Sessions,
691 W., Weber, R. J., Weinheimer, A. J., Wisthaler, A., and Jimenez, J. L.: Effects of aging on organic aerosol from
692 open biomass burning smoke in aircraft and laboratory studies, Atmos. Chem. Phys, 11, 12049-12064, 2011.

693 Dall'Osto, M., Hellebust, S., Healy, R. M., O'Connor, I. P., Kourtchev, I., Sodeau, J. R., Ovadnevaite, J., Ceburnis,
694 D., O'Dowd, C. D., and Wenger, J. C.: Apportionment of urban aerosol sources in Cork (Ireland) by synergistic
695 measurement techniques, Sci. Total Environ, 493, 197-208, 2014.

696 Drewnick, F., Hings, S. S., DeCarlo, P., Jayne, J. T., Gonin, M., Fuhrer, K., Weimer, S., Jimenez, J. L., Demerjian,
697 K. L., Borrmann, S., and Worsnop, D. R.: A new time-of-flight aerosol mass spectrometer (TOF-AMS) - Instrument
698 description and first field deployment, Aerosol Sci. Technol., 39, 637-658, 2005.

699 Engling, G., He, J., Betha, R., and Balasubramanian, R.: Assessing the regional impact of Indonesian biomass
700 burning emissions based on organic molecular tracers and chemical mass balance modeling, Atmos. Chem. Phys,
701 14, 8043-8054, 2014.

702 Fujii, Y., Tohno, S., Amil, N., and Latif, M. T.: Quantitative assessment of source contributions to PM2.5 on the
703 west coast of Peninsular Malaysia to determine the burden of Indonesian peatland fire, Atmos. Environ., 171, 111-
704 117, 10.1016/j.atmosenv.2017.10.009, 2017.

705 Gao, S., Hegg, D. A., Hobbs, P. V., Kirchstetter, T. W., Magi, B. I., and Sadilek, M.: Water-soluble organic
706 components in aerosols associated with savanna fires in southern Africa: Identification, evolution and distribution,
707 Journal of Geophysical Research, 108, SAF27-21-SAF27-16, doi:10.1029/2002JD002324, 2003.

708 Geron, C., and Hays, M.: Air emissions from organic soil burning on the coastal plain of North Carolina, Atmos.
709 Environ., 64, 192-199, 2013.

710 Goulding, K. W. T., Bailey, N., Bradbury, N. J., Hargreaves, P., Howe, M., Murphy, D. V., Poulton, P. R., and
711 Willison, T. W.: Nitrogen deposition and its contribution to nitrogen cycling and associated soil processes, New
712 Phytologist, 139, 49-58, 1998.

713 Grosjean, D.: Wall loss of gaseous pollutants in outdoor Teflon chambers, Environ. Sci. Technol., 19, 1059-1065,
714 10.1021/es00141a006, 1985.

715 Gruber, N., and Galloway, J. N.: An Earth-system prespective of the global nitrogen cycle, Nature, 451, 293-296,
716 2008.

717 Hatch, L. E., Luo, W., Pankow, J. F., Yokelson, R. J., Stockwell, C. E., and Barsanti, K. C.: Identification and
718 quantification of gaseous organic compounds emitted from biomass burning using two-dimensional gas
719 chromatography-time-of-flight mass spectrometry, Atmos. Chem. Phys, 15, 1865-1899, 2015.

720 Heil, A., and Goldammer, J. G.: Smoke-haze pollution: a review of the 1997 episode in Southeast Asia, Regional
721 Environmental Change, 2, 24-37, 2001.

722 Hennigan, C. J., Sullivan, A. P., Collett Jr., J. L., and Ronbinson, A. L.: Levoglucosan stability in biomass burning
723 particles exposed to hydroxyl radicals, Geophysical Research Letters, 37, 1-4, 2010.

724 Hibbard, T., and Killard, J.: Breath ammonia levels in a normal human population study as determined by
725 photoacoustic laser spectroscopy, Juornal of Breath Research, 5, 1-8, 2011.

726 Hinds, W. C.: Aerosol Technology: Properties, Behavior, and Measurement of Airborne Particles, 2nd Ed., 2nd ed.,
727 John Wiley and Sons, Inc., New York, NY, 1999.

Hoffmann, D., Tilgner, A., Iinuma, Y., and Herrmann, H.: Atmospheric stability of levoglucosan: A detailed laboratory and modeling study, Environ. Sci. Technol., 44, 694-699, 2010.

Hu, Y. Q., Fernandez-Anez, N., Smith, T. E. L., and Rein, G.: Review of emissions from smouldering peat fires and their contribution to regional haze episodes, International Journal of Wildland Fire, 27, 293-312, 10.1071/wf17084, 2018.

Hu, Y. Q., Christensen, E., Restuccia, F., and Rein, G.: Transient gas and particle emissions from smouldering combustion of peat, Proceedings of the Combustion Institute, 37, 4035-4042, 10.1016/j.proci.2018.06.008, 2019.

Huijnen, V., Wooster, M. J., Kaiser, J. W., Gaveau, D. L. A., Flemming, J., Parrington, M., Inness, A., Murdiyarso, D., Main, B., and van Weele, M.: Fire carbon emissions over maritime southeast Asia in 2015 largest since 1997, Scientific Reports, 6, 10.1038/srep26886, 2016.

Iinuma, Y., Bruggemann, E., Gnauk, T., Muller, K., Andreae, M. O., Helas, G., Parmar, R., and Herrmann, H.: Source characterization of biomass burning particles: The combustion of selected European conifers, African hardwood, savanna grass, and German and Indonesian peat, J. Geophys. Res. Atmos., 112, 2007.

IPCC: 2013 supplement to th 2006 IPCC guidelines for national greenhouse gas inventories: Wetlands, Switzerland, 2014. https://www.ipcc.ch/site/assets/uploads/2018/03/Wetlands_Supplement_Entire_Report.pdf

Jaakkola, P. T., Vahlman, T. A., Roos, A. A., Saarinen, P. E., and Kauppinen, J. K.: On-line analysis of stack gas composition by a low resolution FT-IR gas analyzer, Water Air and Soil Pollution, 101, 79-92, 1998.

Jayarathne, T., Stockwell, C. E., Gilbert, A. A., Daugherty, K., Cochrane, M. A., Ryan, K. C., Putra, E. I., Saharjo, B. H., Nurhayati, A. D., Albar, I., Yokelson, R. J., and Stone, E. A.: Chemical characterization of fine particulate matter emitted by peat fires in Central Kalimantan, Indonesia, during the 2015 El Nino, Atmos. Chem. Phys, 18, 2585-2600, 10.5194/acp-18-2585-2018, 2018.

Jickells, T., Baker, A. R., Cape, J. N., Cornell, S. E., and Nemitz, E.: The cycling of organic nitrogen through the atmosphere, Philosophical Transactions: Biological Sciences, 368, 1-7, 2013.

Karjalainen, P., Timonen, H., Saukko, E., Kuuluvainen, H., Saarikoski, S., Aakko-Saksa, P., Murtonen, T., Bloss, M., Dal Maso, M., Simonen, P., Ahlberg, E., Svenningsson, B., Brune, W. H., Hillamo, R., Keskinen, J., and Ronkko, T.: Time-resolved characterization of primary particle emissions and secondary particle formation from a modern gasoline passenger car, Atmos. Chem. Phys, 16, 8559-8570, 10.5194/acp-16-8559-2016, 2016.

Kleinman, L. I., Daum, P. H., Lee, Y.-N., Nunnermacker, L. J., Springston, S. R., Weinstein-Lloyd, J., Hyde, P., Doskey, P. V., Rudolph, J., Fast, J., and Berkowitz, C.: Photochemical age determinations in the Phoenix metropolitan area, Journal of Geophysical Research, 108, 2003.

Kleinman, L. I., Daum, P. H., Lee, Y. N., Senum, G. I., Springston, S. R., Wang, J., Berkowitz, C., Hubbe, J., Zaveri, R. A., Brechtel, F. J., Jayne, J., Onasch, T. B., and Worsnop, D. R.: Aircraft observations of aerosol composition and ageing in New England and Mid-Atlantic States during the summer 2002 New England Air Quality Study field campaign, J. Geophys. Res. Atmos., 112, 2007.

Kopacek, J., and Posch, M.: Anthropogenic nitrogen emissions during the Holocene and their possible effects on remote ecosystems, Global Biogeochemical Cycles, 25, 1-17, 2011.

Koppmann, R., von Czapiewski, K., and Reid, J. S.: A review of biomass burning emissions, part 1: gaseous emissions of carbon monoxide, methane, volatile organic compounds, and nitrogen containing compounds, Atmospheric Chemistry and Physics Discussion, 5, 10455-10516, 2005.

Koss, A. R., Sekimoto, K., Gilman, J. B., Selimovic, V., Coggon, M. M., Zarzana, K. J., Yuan, B., Lerner, B. M., Brown, S. S., Jimenez, J. L., Krechmer, J., Roberts, J. M., Warneke, C., Yokelson, R. J., and de Gouw, J.: Non-

769 methane organic gas emissions from biomass burning: identification, quantification, and emission factors from PTR-
770 ToF during the FIREX 2016 laboratory experiment, Atmos. Chem. Phys., 18, 3299-3319, 10.5194/acp-18-3299-
771 2018, 2018.

772 Kuhlbusch, T. A., Lobert, J. M., Crutzen, P. J., and Warneck, P.: Molecular nitrogen emissions from denitrification
773 during biomass burning, Nature, 351, 135-137, 1991.

774 Kundu, S., Kawamura, K., Andreae, T. W., Hoffer, A., and Andreae, M. O.: Molecular distributions of dicarboxylic
775 acids, ketocarboxylic acids and alpha-dicarbonyls in biomass burning aerosols: implications for photochemical
776 production and degradation in smoke layers, Atmos. Chem. Phys, 10, 2209-2225, 2010.

777 Kuwata, M., Neelam-Naganathan, G. G., Miyakawa, T., Khan, M. F., Kozan, O., Kawasaki, M., Sumin, S., and
778 Latif, M. T.: Constraining the emission of particulate matter from Indonesian peatland burning using continuous
779 observation data, J. Geophys. Res. Atmos., 123, 9828-9842, 10.1029/2018jd028564, 2018.

780 Lai, C. Y., Liu, Y. C., Ma, J. Z., Ma, Q. X., and He, H.: Degradation kinetics of levoglucosan initiated by hydroxyl
781 radical under different environmental conditions, Atmos. Environ., 91, 32-39, 2014.

782 Lambe, A. T., Ahern, A. T., Williams, L. R., Slowik, J. G., Wong, J. P. S., Abbatt, J. P. D., Brune, W. H., Ng, N. L.,
783 Wright, J. P., Croasdale, D. R., Worsnop, D. R., Davidovits, P., and Onasch, T. B.: Characterization of aerosol
784 photooxidation flow reactors: heterogeneous oxidation, secondary organic aerosol formation and cloud condensation
785 nuclei activity measurements, Atmos. Meas. Tech., 4, 445-461, 10.5194/amt-4-445-2011, 2011.

786 Laskin, A., Smith, J. S., and Laskin, J.: Molecular Characterization of Nitrogen-Containing Organic Compounds in
787 Biomass Burning Aerosols Using High-Resolution Mass Spectrometry, Environ. Sci. Technol., 43, 3764-3771,
788 2009.

789 Levine, J. S.: The 1997 fires in Kalimantan and Sumatra, Indonesia: Gaseous and particulate emissions,
790 Geophysical Research Letters, 26, 815-818, 1999.

791 Li, Q., Jacob, B. D. J., Bey, I., Yantosca, R. M., Zhao, Y. J., Kondo, Y., and Notholt, J.: Atmospheric hydrogen
792 cyanide (HCN): Biomass burning source, ocean sink?, Geophysical Research Letters, 27, 357-360, 2000.

793 Li, R., Palm, B. B., Ortega, A. M., Hlywiak, J., Hu, W., Peng, Z., Day, D. A., Knote, C., Brune, W. H., de Gouw, J.
794 A., and Jimenez, J. L.: Modeling the Radical Chemistry in an Oxidation Flow Reactor: Radical Formation and
795 Recycling, Sensitivities, and the OH Exposure Estimation Equation, The Journal of Physical Chemistry A, 119,
796 4418-4432, 10.1021/jp509534k, 2015.

797 Lobert, J. M., Scharffe, D. H., Hao, W. M., and Crutzen, P. J.: Importance of biomass burning in the atmopsheric
798 budgets of nitrogen-containing gases, Nature, 346, 552-554, 1990.

799 May, A. A., Saleh, R., Hennigan, C. J., Donahue, N. M., and Robinson, A. L.: Volatility of organic molecular
800 markers used for source apportionment analysis: Measurements and implications for atmospheric lifetime, Environ.
801 Sci. Technol., 46, 12435-12444, 2012.

802 May, A. A., McMeeking, G. R., Lee, T., Taylor, J. W., Craven, J. S., Burling, I., Sullivan, A. P., Akagi, S., Collett,
803 J. L., Flynn, M., Coe, H., Urbanski, S. P., Seinfeld, J. H., Yokelson, R. J., and Kreidenweis, S. M.: Aerosol
804 emissions from prescribed fires in the United States: A synthesis of laboratory and aircraft measurements, J.
805 Geophys. Res. Atmos., 119, 11826-11849, 2014.

806 McMahon, C. K., Wade, D. D., and Tsoukalas, S. N.: Combustion characteristics and emissions from burning
807 organic soils, in: Proceedings, 73rd Annual Meeting of the Air Pollution Control Association, Air & Waste
808 Management Association, Pittsburgh, PA, 1980.

McMurry, P. H., and Grosjean, D.: Gas and aerosol wall losses in Teflon film smog chambers, Environ. Sci. Technol., 19, 1176-1182, 10.1021/es00142a006, 1985.

Miettinen, J., Hooijer, A., Vernimmen, R., Liew, S. C., and Page, S. E.: From carbon sink to carbon source: Extensive peat oxidation in insular Southeast Asia since 1990, Environmental Research Letters, 12, 2017.

Muraleedharan, T. R., Radojevic, M., Waugh, A., and Caruana, A.: Emissions from the combustion of peat: An experimental study, Atmos. Environ., 34, 3033-3035, 2000.

Na, K., Song, C., Switzer, C., and Cocker, D. R.: Effect of ammonia on secondary organic aerosol formation from alpha-Pinene ozonolysis in dry and humid conditions, Environ. Sci. Technol., 41, 6096-6102, 2007.

Nara, H., Tanimoto, H., Tohjima, Y., Mukai, H., Nojiri, Y., and Machida, T.: Emission factors of CO_2, CO and CH_4 from Sumatran peatland fires in 2013 based on shipboard measurements, Tellus Series B-Chemical and Physical Meteorology, 69, 10.1080/16000889.2017.1399047, 2017.

Neff, J. C., Holland, E. A., Dentener, F. J., McDowell, W. H., and Russell, K. M.: The origin, composition and rates of organic nitrogen deposition: a missing piece of the nitrogen cycle?, Biogeochemistry, 57/58, 99-136, 2002.

Neuman, J. A., Huey, L. G., Ryerson, T. B., and Fahey, D. W.: Study of Inlet Materials for Sampling Atmospheric Nitric Acid, Environ. Sci. Technol., 33, 1133-1136, 10.1021/es980767f, 1999.

Ng, N. L., Chhabra, P. S., Chan, A. W. H., Surratt, J. D., Kroll, J. H., Kwan, A. J., McCabe, D. C., Wennberg, P. O., Sorooshian, A., Murphy, S. M., Dalleska, N. F., Flagan, R. C., and Seinfeld, J. H.: Effect of NOx level on secondary organic aerosol (SOA) formation from the photooxidation of terpenes, Atmos. Chem. Phys, 7, 5159-5174, 2007.

NIOSH: Method 5050, Elemental carbon (diesel particulate), in: NIOSH Manual of Analytical Methods, 4th ed. ed., National Institute of Occupational Safety and Health, Cincinnati, OH, 1999.

Ohlemiller, T. J., Bellan, J., and Rogers, F.: A model of smoldering combustion applied to flexible polyurethane foams, Combustion and Flame, 36, 197-215, 1979.

Olszyna, K. J., Bailey, E. M., Simonaitis, R., and Meagher, J. F.: O_3 and NO_y relationships at a rural site, Journal of Geophysical Research, 99, 14557-14563, 1994.

Page, S. E., Siegert, F., Rieley, J. O., Boehm, H. D. V., Jaya, A., and Limin, S.: The amount of carbon released from peat and forest fires in Indonesia during 1997, Nature, 420, 61-65, 10.1038/nature01131, 2002.

Page, S. E., Rieley, J. O., and Banks, C. J.: Global and regional importance of the tropical peatland carbon pool, Global Change Biology, 17, 798-818, 2011.

Parrish, D. D., Hahn, C. J., Williams, E. J., Norton, E. B., and Fehsenfeld, F. C.: Indications of photochemical histories of Pacific air masses from measurements of atmospheric trace species at Point Arena, California, Journal of Geophysical Research Letters, 97, 15833-15901, 1992.

Peng, Z., Day, D. A., Stark, H., Li, R., Lee-Taylor, J., Palm, B. B., Brune, W. H., and Jimenez, J. L.: HO_x radical chemistry in oxidation flow reactors with low-pressure mercury lamps systematically examined by modeling, Atmos. Meas. Tech., 8, 4863-4890, 10.5194/amt-8-4863-2015, 2015.

Pokhrel, R. P., Wagner, N. L., Langridge, J. M., Lack, D. A., Jayarathne, T., Stone, E. A., Stockwell, C. E., Yokelson, R. J., and Murphy, S. M.: Parameterization of single-scattering albedo (SSA) and absorption Angstrom exponent (AAE) with EC /OC for aerosol emissions from biomass burning, Atmos. Chem. Phys, 16, 9549-9561, 10.5194/acp-16-9549-2016, 2016.

Pratap, V., Bian, Q. J., Kiran, S. A., Hopke, P. K., Pierce, J. R., and Nakao, S.: Investigation of levoglucosan decay in wood smoke smog-chamber experiments: The importance of aerosol loading, temperature, and vapor wall losses in interpreting results, Atmos. Environ., 199, 224-232, 10.1016/j.atmosenv.2018.11.020, 2019.

Prenni, A. J., Levin, E. J. T., Benedict, K. B., Sullivan, A. P., Schurman, M. I., Gebhart, K. A., Day, D. E., Carrico, C. M., Malm, W. C., Schichtel, B. A., Collett, J. L., and Kreidenweis, S. M.: Gas-phase reactive nitrogen near Grand Teton National Park: Impacts of transport, anthropogenic emissions, and biomass burning, Atmos. Environ., 89, 749-756, 2014.

Rein, G., Cohen, S., and Simeoni, A.: Carbon emissions from smouldering peat in shallow and strong fronts, Proceedings of the Combustion Institute, 32, 2489-2496, 0.1016/j.proci.2008.07.008, 2009.

Roberts, J. M., Veres, P. R., Cochran, A. K., Warneke, C., Burling, I. R., Yokelson, R. J., Lerner, B., Gilman, J. B., Kuster, W. C., Fall, R., and de Gouw, J.: Isocyanic acid in the atmosphere and its possible link to smoke-related health effects, Proc. Natl. Acad. Sci. USA, 108, 8966-8971, 2011.

Roulston, C., Paton-Walsh, C., Smith, T. E. L., Guerette, E. A., Evers, S., Yule, C. M., Rein, G., and Van der Werf, G. R.: Fine particle emissions from tropical peat fires decrease rapidly with time since ignition, J. Geophys. Res. Atmos., 123, 5607-5617, 10.1029/2017jd027827, 2018.

Seinfeld, J. H., and Pandis, S. N.: Atmospheric Chemistry and Physics: From Air Pollution to Climate Change, John Wiley & Sons, New York, NY, 1998.

Setyawati, W., Damanhuri, E., Lestari, P., and Dewi, K.: Emission factor from small scale tropical peat combustion, in: 1st Annual Applied Science and Engineering Conference, edited by: Abdullah, A. G., Nandiyanto, A. B. D., and Danuwijaya, A. A., IOP Conference Series-Materials Science and Engineering, 2017.

Simoneit, B. R. T., Rushdi, A. I., Bin Abas, M. R., and Didyk, B. M.: Alkyl amides and nitriles as novel tracers for biomass burning, Environ. Sci. Technol., 37, 16-21, 2003.

Smith, T. E. L., Evers, S., Yule, C. M., and Gan, J. Y.: In situ tropical peatland fire emission factors and their variability, as determined by field measurements in peninsula Malaysia, Global Biogeochemical Cycles, 32, 18-31, 10.1002/2017gb005709, 2018.

Stephens, M., Turner, N., and Sandberg, J.: Particle identification by laser-induced incandescence in a solid-state laser cavity, Appl. Opt., 42, 3726-3736, 10.1364/ao.42.003726, 2003.

Stockwell, C. E., Yokelson, R. J., Kreidenweis, S. M., Robinson, A. L., Demott, P. J., Sullivan, R. C., Reardon, J., Ryan, K. C., Griffith, D. W. T., and Stevens, L.: Trace gas emissions from combustion of peat, crop residue, domestic biofuels, grasses, and other fuels: configuration and Fourier transform infrared (FTIR) component of the fourth Fire Lab at Missoula Experiment (FLAME-4), Atmos. Chem. Phys, 14, 9727-9754, 2014.

Stockwell, C. E., Veres, P. R., Williams, J., and Yokelson, R. J.: Characterization of biomass burning emissions from cooking fires, peat, crop residue, and other fuels with high-resolution proton-transfer-reaction time-of-flight mass spectrometry, Atmos. Chem. Phys, 15, 845-865, 2015.

Stockwell, C. E., Jayarathne, T., Cochrane, M. A., Ryan, K. C., Putra, E. I., Saharjo, B. H., Nurhayati, A. D., Albar, I., Blake, D. R., Simpson, I. J., Stone, E. A., and Yokelson, R. J.: Field measurements of trace gases and aerosols emitted by peat fires in Central Kalimantan, Indonesia, during the 2015 El Nino, Atmos. Chem. Phys, 16, 11711-11732, 10.5194/acp-16-11711-2016, 2016.

Tham, J., Sarkar, S., Jia, S. G., Reid, J. S., Mishra, S., Sudiana, I. M., Swarup, S., Ong, C. N., and Yu, L. Y. E.: Impacts of peat-forest smoke on urban PM2.5 in the Maritime Continent during 2012-2015: Carbonaceous profiles and indicators, Environ. Pollut., 248, 496-505, 10.1016/j.envpol.2019.02.049, 2019.

Tian, J., Chow, J. C., Cao, J. J., Han, Y. M., Ni, H. Y., Chen, L.-W. A., Wang, X. L., Huang, R. J., Moosmüller, H., and Watson, J. G.: A biomass combustion chamber: Design, evaluation, and a case study of wheat straw combustion emission tests, Aerosol Air Qual. Res., 15, 2104-2114, 2015.

Turetsky, M. R., Kane, E. S., Harden, J. W., Ottmar, R. D., Manies, K. L., Hoy, E., and Kasischke, E. S.: Recent acceleration of biomass burning and carbon losses in Alaskan forests and peatlands, Nature Geoscience, 4, 27-31, 2010.

Turetsky, M. R., Benscoter, B., Page, S., Rein, G., van der Werf, G. R., and Watts, A.: Global vulnerability of peatlands to fire and carbon loss, Nature Geoscience, 8, 11-14, 10.1038/ngeo2325, 2015a.

Turetsky, M. R., Benscoter, B., Page, S. E., Rein, G., van der Werf, G. R., and Watts, A. C.: Controls on global peat fires and consequences for the carbon cycle, Nature, 2015b.

Updyke, K. M., Nguyen, T. B., and Nizkorodov, S. A.: Formation of brown carbon via reactions of ammonia with secondary organic aerosols from biogenic and anthropogenic precursors, Atmos. Environ., 63, 22-31, 2012.

VDI: Measurement of soot (ambient air) - Thermographic determination of elemental carbon after thermal desorption of organic carbon, Verein Deutscher Ingenieure, Dusseldorf, Germany, 1999.

Villena, G., Bejan, I., Kurtenbach, R., Wiesen, P., and Kleffmann, J.: Interferences of commercial NO_2 instruments in the urban atmosphere and in a smog chamber, Atmos. Meas. Tech., 5, 149-159, 2012.

Wang, N. X., Jorga, S. D., Pierce, J. R., Donahue, N. M., and Pandis, S. N.: Particle wall-loss correction methods in smog chamber experiments, Atmos. Meas. Tech., 11, 6577-6588, 10.5194/amt-11-6577-2018, 2018.

Wang, X. L., Chancellor, G., Evenstad, J., Farnsworth, J. E., Hase, A., Olson, G. M., Sreenath, A., and Agarwal, J. K.: A novel optical instrument for estimating size segregated aerosol mass concentration in real time, Aerosol Sci. Technol., 43, 939-950, 2009.

Wang, X. L., Watson, J. G., Chow, J. C., Gronstal, S., and Kohl, S. D.: An efficient multipollutant system for measuring real-world emissions from stationary and mobile sources, Aerosol Air Qual. Res., 12, 145-160, 2012.

Ward, D. E., and Hardy, C. C.: Advances in the characterization and control of emissions from prescribed fires, 77th Annual Meeting of the Air pollution Control Association, San Francisco, CA, 1984.

Ward, D. E., and Radke, L. F.: Emissions measurements from vegetation fires: A comparative evaluation of methods and results, Fire in the Environment: The Ecological, Atmospheric and Climatic Importance of Vegetation Fires, 13, 53-76, 1993.

Watson, J. G., Chow, J. C., and Frazier, C. A.: X-ray fluorescence analysis of ambient air samples, in: Elemental Analysis of Airborne Particles, Vol. 1, edited by: Landsberger, S., and Creatchman, M., Advances in Environmental, Industrial and Process Control Technologies, Gordon and Breach Science, Amsterdam, The Netherlands, 67-96, 1999.

Watson, J. G., Tropp, R. J., Kohl, S. D., Wang, X. L., and Chow, J. C.: Filter processing and gravimetric analysis for suspended particulate matter samples, Aerosol Science and Engineering, 1, 193-205, 2017.

Watts, A. C.: Organic soil combustion in cypress swamps: Moisture effects and landscape implications for carbon release, Forest Ecology and Management, 294, 178-187, 10.1016/j.foreco.2012.07.032, 2013.

Wilson, D., Dixon, S. D., Artz, R. R. E., Smith, T. E. L., Evans, C. D., Owen, H. J. F., Archer, E., and Renou-Wilson, F.: Derivation of greenhouse gas emission factors for peatlands managed for extraction in the Republic of Ireland and the United Kingdom, Biogeosciences, 12, 5291-5308, 2015.

Winer, A. M., Peters, J. W., Smith, J. P., and Pitts, J. N., Jr.: Response of commercial chemiluminescence NO-NO_2 analyzers to other nitrogen-containing compounds, Environ. Sci. Technol., 8, 1118-1121, 1974.

Wooster, M. J., Gaveau, D. L. A., Salim, M. A., Zhang, T. R., Xu, W. D., Green, D. C., Huijnen, V., Murdiyarso, D., Gunawan, D., Borchard, N., Schirrmann, M., Main, B., and Sepriando, A.: New tropical peatland gas and particulate emissions factors indicate 2015 Indonesian fires released far more particulate matter (but less methane) than current inventories imply, Remote Sensing, 10, 10.3390/rs10040495, 2018.

Yatavelli, R. L. N., Chen, L.-W. A., Knue, J., Samburova, V., Gyawali, M., Watts, A. C., Chakrabarty, R. K., Moosmuller, H., Hodzic, A., Wang, X. L., Zielinska, B., Chow, J. C., and Watson, J. G.: Emissions and partitioning of intermediate-volatility and semi-volatile polar organic compounds (I/SV-POCs) during laboratory combustion of boreal and sub-tropical peat, Aerosol Science and Engineering, 1, 25-32, 2017.

Yokelson, R. J., Susott, R., Ward, D. E., Reardon, J., and Griffith, D. W. T.: Emissions from smoldering combustion of biomass measured by open- path Fourier transform infrared spectroscopy, Journal of Geophysical Research, 102, 18865-18877, 1997.

Yokelson, R. J., Burling, I. R., Gilman, J. B., Warneke, C., Stockwell, C. E., de Gouw, J., Akagi, S. K., Urbanski, S. P., Veres, P., Roberts, J. M., Kuster, W. C., Reardon, J., Griffith, D. W. T., Johnson, T. J., Hosseini, S., Miller, J. W., Cocker, D. R., Jung, H., and Weise, D. R.: Coupling field and laboratory measurements to estimate the emission factors of identified and unidentified trace gases for prescribed fires, Atmos. Chem. Phys, 13, 89-116, 2013.

Yu, Z. C., Loisel, J., Brosseau, D. P., Beilman, D. W., and Hunt, S. J.: Global peatland dynamics since the Last Glacial Maximum, Geophysical Research Letters, 37, 10.1029/2010gl043584, 2010.

Zhao, Y. L., Kreisberg, N. M., Worton, D. R., Isaacman, G., Weber, R. J., Liu, S., Day, D. A., Russell, L. M., Markovic, M. Z., VandenBoer, T. C., Murphy, J. G., Hering, S. V., and Goldstein, A. H.: Insights into secondary organic aerosol formation mechanisms from measured gas/particle partitioning of specific organic tracer compounds, Environ. Sci. Technol., 47, 3781-3787, 2013.

Table 1. Average peat composition[a] (dry weight percentage) for total carbon (C), hydrogen (H), nitrogen (N), sulfur (S), and oxygen (O).

Peat Location	C (%)	H (%)	N (%)	S (%)	O (%)	N/C mass ratio	Sum (CHNSO; %)
Odintsovo, Russia	44.20 ± 1.01	6.43 ± 0.16	1.50 ± 0.52	<0.01	38.64 ± 0.78	0.034	90.8
Pskov, Siberia	52.03 ± 0.23	6.30 ± 0.05	2.92 ± 0.12	<0.01	36.83 ± 0.39	0.056	98.1
Northern Alaska, USA	50.94 ± 0.81	6.05 ± 0.07	1.79 ± 0.09	<0.01	36.62 ± 0.30	0.035	95.4
Putnam County Lakebed, Florida, USA	56.64 ± 0.37	6.25 ± 0.40	3.53 ± 0.05	<0.01	31.43 ± 0.36	0.062	97.8
Everglades, Florida, USA	47.22 ± 0.57	5.15 ± 0.16	3.93 ± 0.08	<0.01	34.18 ± 0.87	0.083	90.5
Caohai, Guizhou, Southeast China	19.74 ± 2.01	2.09 ± 1.26	1.35 ± 0.16	<0.01	23.95 ± 1.15	0.068	47.1
Gaopo, Guizhou, Southeast China	29.70 ± 2.09	3.13 ± 0.16	2.08 ± 0.22	<0.01	21.46 ± 1.27	0.070	56.4
Borneo, Malaysia	50.55 ± 2.53	6.46 ± 0.99	1.16 ± 0.08	<0.01	33.72 ± 0.30	0.023	91.9

[a]Elemental analyses were performed using Elemental Analyzer (Flash EA1112 CHNS/O Analyzer, Thermo Fisher Scientific, Waltham, MA, USA). Each dried peat sample (~2–3 g) was submitted for combustion analysis at 900°C for C, H, N, and S in a helium/oxygen atmosphere and at 1060°C for O in a helium atmosphere. Three to four replicate sample analyses were conducted for each type of peat to obtain the average and standard deviations.

Table 2. Peat combustion emission factors (EFs) for CO_2, CO, and CH_4[a].

Sampling Location or Review (Reference)	Sampling Method (No. of samples)[b]	Modified Combustion Efficiency (MCE)	Measurement Method	Average Emission Factors (g/kg)			Ratio (EF_{CO}/EF_{CO2})
				EF_{CO2}	EF_{CO}	EF_{CH4}	
Boreal							
Odintsovo, Russia	Lab	0.81 ± 0.03	CO/CO_2 monitors	1073 ± 63	157 ± 24	3.20 ± 0.69	0.15
(This study)	(n=6, 25 % FM[c])		and FTIR[d]				
Pskov, Siberia	Lab	0.85 ± 0.01	CO/CO_2 monitors	1380 ± 27	159 ± 14	6.94 ± 1.48	0.12
(This study)	(n=7, 25 % FM[c])		and FTIR[d]				
Western Siberia	Lab	Smoldering	CO/CO_2 monitors				
(Chakrabarty et al., 2016)	(n=1, 25 % FM[c])			1432	204	NA	0.14
	(n=1, 50 % FM[c])			1698	49		0.029
Temperate							
Northern Alaska, USA	Lab	0.86 ± 0.03	CO/CO_2 monitors	1400 ± 38	161 ± 19	5.69 ± 1.07	0.12
(This study)	(n=6, 25 % FM[c])		and FTIR[d]				
Northern Alaska, USA	Lab	Smoldering	CO/CO_2 monitors				
(Chakrabarty et al., 2016)	(n=1, 25 % FM[c])			1238	83	NA	0.067
	(n=1, 50 % FM[c])			1598	128		0.08
Hudson Bay lowland, Ontario, Canada	Lab	0.81 ± 0.009	FTIR	1274 ± 19	197 ± 9	6.25 ± 2.17	0.15
(Stockwell et al., 2014)							
Alaska and Minnesota, USA	Lab	0.81 ± 0.327	FTIR	1395 ± 52[e]	209 ± 68[e]	6.85 ± 5.66[e]	0.15
(Yokelson et al., 1997)							
Edinburg, Scotland, UK	Lab	Smoldering	Infrared system	420 ± 134	170 ± 33	NA	0.40
(Rein et al., 2009)							
Sphagnum moss peat, Ireland	Lab	0.84 ± 0.019	FTIR	1346 ± 31	218 ± 22	8.35 ± 1.3	0.16
(Wilson et al., 2015)	(n=5)						
Subtropical							
Putnam County Lakebed, FL, USA	Lab		CO/CO_2 monitors				
(This study)	(n=6, 25 % FM[c])	0.65 ± 0.04	and FTIR[d]	1126 ± 89	394 ± 46	10.42 ± 1.81	0.35
	(n=3, 60 % FM[c])	0.72 ± 0.01		1262 ± 27	315 ± 10	9.18 ± 0.26	0.25
Everglades National Park, FL, USA	Lab	0.90 ± 0.03	CO/CO_2 monitors	1292 ± 80	93 ± 21	7.65 ± 1.36	0.07

(This study)	(n=3, 25 % FM[e])	(mix of flaming and smoldering)	and FTIR[d]				
Pocosin Lake NWR[f], NC, USA (Geron and Hays, 2013)	Field (Feb & Aug 2008) (n=3)	0.77–0.83	CO and Infrared gas monitoring	1010–1140	230–300	NA	NA
Green Swamp Preserve, NC, USA (Geron and Hays, 2013))	Field (Feb 2009) (n=8)	0.80–0.81	CO and Infrared gas monitoring	1100–1640	10–280	NA	NA
Alligator River (AR) NWR[f], NC, USA (Geron and Hays, 2013)	Field (May 2011) (n=8)	0.79-0.86	CO and Infrared gas monitoring	1092–1440	125–290	NA	NA
Pocosin Lake NWR[f], NC, USA (Black et al., 2016)	Lab (n=2)	0.83 ± 0.02	CO/CO_2 monitors	922 ± 47	122 ± 14	NA	0.13
Alligator River NWR[f], NC, USA (Black et al., 2016)	Lab (n=2)	0.86 ± 0.02	CO/CO_2 monitors	861 ± 112	108 ± 20	NA	0.13
Tropical							
Borneo, Malaysia (This study)	Lab (n=6, 25 % FM[e])	0.85 ± 0.02	CO/CO_2 monitors and FTIR[d]	1331 ± 78	171 ± 22	6.65 ± 0.93	0.13
Peninsula, Malaysia (Smith et al., 2018)	Field (Aug 2015) (n=10)	0.80 ± 0.03	FTIR	1579 ± 58	251 ± 39	11 ± 6.1	0.16
Central Kalimantan, Indonesia (Wooster et al., 2018)	Field (Sep/Oct 2015) (n=23)	0.81 ± 0.032	Cavity-enhanced laser absorption spectrometer and FTIR	1775 ± 64	279 ± 44	7.9 ± 2.4	0.16
Central Kalimantan, Indonesia[j] (Stockwell et al., 2016)	Field (Oct/Nov 2015) (n=35)	0.77 ± 0.053	FTIR	1564 ± 77	291 ± 49	9.51 ± 4.74	0.19
Central Kalimantan, Indonesia (Huijnen et al., 2016)	Field (Oct 2015)	0.8	Cavity-ring down spectrometer	1594 ± 61	255 ± 39	7.4 ± 2.3	0.16
West Kalimantan, Indonesia	Lab	Flaming (0.998 ± 0.005)	CO/CO_2 monitors	2088 ± 21	3.10 ± 7.17	0.14 ± 0.13	0.0015

(Setyawati et al., 2017)	(n=17 each)	Smoldering (0.89 ± 0.06)	and gas chromatography	1831 ± 131	138 ± 72	17 ± 1.2	0.075
South Kalimantan, Indonesia (Stockwell et al., 2014)	Lab (n=3)	0.82 ± 0.065	FTIR	1637 ± 204	233 ± 72	12.8 ± 6.61	0.14
South Sumatra, Indonesia (Christian et al., 2003)	Lab (n=1)	0.84	FTIR	1703	210	20.8	0.12
North-Central Sumatra, Indonesia (Nara et al., 2017)	Shipboard (June-Aug 2013) (n=5)	0.84	Infrared and cavity ring-down spectrometer	1663 ± 54	205 ± 23	7.6 ± 1.6	0.12
Reviews[g]							
Atmospheric Modeling (Akagi et al., 2011)	NA	NA	NA	1563 ± 65	182 ± 60	11.8 ± 7.8	0.12
Boreal/Temperate				1327 ± 150[h]	207 ± 70[h]	9 ± 4[h]	NA
Tropical	NA	NA	NA	1703[i]	210[i]	21[i]	NA
(IPCC, 2014)							
Boreal/Temperate	NA	Smoldering	NA	1134 ± 139	179 ± 61	8.1 ± 4.1	0.16
Tropical				1615 ± 184	248 ± 50	12.3 ± 5.0	0.40
(Hu et al., 2018)							
Peat Fire (Andreae, 2019)	NA	NA	NA	1550 ± 130	250 ± 23	9.3 ± 1.5	0.45

[a]Data acquired from this study are highlighted in green
[b]Only included number of samples reported
[c]FM; Fuel moisture content
[d]FTIR: Fourier transform infrared spectroscopy. CH_4 was acquired by FTIR in this study
[e]Obtained from Stockwell et al. (2014) as only the ratios of moles compound/total moles carbon detected was reported in Yokelson et al. (1997)
[f]NWR: National Wildlife Reserve
[g]Reviews for atmospheric modeling and emission inventory development
[h]From Ward and Hardy (1984); Yokelson et al. (1997;2013)
[i]From Christian et al. (2003) for tropical peats
[j]Detailed volatile organic gas emission factors for one of these samples are reported by Koss et al. (2018)

Table 3. Peat combustion emission factors (EFs) for gaseous nitrogen species[a].

Sampling Location (Reference)	No. of samples	Average Emission Factors (g/kg)								Percent NO_x/NO_y
		EF_{NH_3}[b]	EF_{HCN}[b]	EF_{NO}[c]	EF_{NO_2}[c]	$EF_{NO_x(as\ NO_2)}$	$EF_{NO_y(as\ NO_2)}$[d]	EF_{N_2O}[b]	EF_{HONO}	
Boreal										
Odintsovo, Russia (This study)	6	0.99 ± 0.47	2.45 ± 0.43	0.34 ± 0.04	0.48 ± 0.11	1.01 ± 0.14	1.06 ± 0.11	1.64 ± 0.32	NA	95 ± 6%
Pskov, Siberia (This study)	7	4.65 ± 1.38	5.00 ± 0.74	0.84 ± 0.12	0.42 ± 0.03	1.70 ± 0.20	2.22 ± 0.27	2.29 ± 0.29	NA	77 ± 5%
Pskov, Siberia (Bhattarai et al., 2018)	3	NA	NA	NA	NA	0.08 ± 0.04[e]	NA	NA	NA	NA
Temperate										
Northern Alaska, USA (This study)	6	2.7 ± 0.62	2.33 ± 0.22	0.84 ± 0.44	0.37 ± 0.13	1.67 ± 0.76	2.10 ± 0.85	1.57 ± 0.16	NA	79 ± 9%
Hudson Bay lowland, Ontario, Canada (Stockwell et al., 2014)	NA	2.21 ± 0.24	1.77 ± 0.55	NA	NA	NA	NA	NA	0.18	NA
Alaska and Minnesota, USA (Yokelson et al., 1997)	NA	8.76 ± 13.76	5.09 ± 5.64	NA	NA	NA	NA	NA	NA	NA
Sphagnum moss peat, Ireland (Wilson et al., 2015)	5	2.20 ± 0.35	0.73 ± 0.50	NA	NA	NA	NA	NA	NA	NA
Coastal Swamp land, NC, USA (Stockwell et al., 2014)	NA	1.87 ± 0.37	4.45 ± 3.02	NA	NA	NA	NA	NA	8.48 ± 0.05	NA
Subtropical										
Putnam County Lakebed, FL, USA (This study)	6 (25 % FM)	3.2 ± 0.26	11.5 ± 2.3	1.01 ± 0.33	0.35 ± 0.28	2.01 ± 0.68	2.91 ± 0.34	3.57 ± 0.63	NA	68 ± 15%
	3 (60 % FM)	3.3 ± 0.05	11.7 ± 0.3	0.71 ± 0.07	0.65 ± 0.05	1.74 ± 0.15	2.39 ± 0.19	3.89 ± 0.01	NA	73 ± 5%
Everglades National Park, FL, USA (This study)	6	11.9 ± 2.01	5.12 ± 1.60	1.78 ± 0.31	0.83 ± 0.16	3.56 ± 0.58	4.33 ± 1.10	1.46 ± 0.28	NA	85 ± 14%
Putnam County Lakebed, FL, USA (Bhattarai et al., 2018)		NA	NA	NA	NA	0.11 ± 0.05[e]	NA	NA	NA	73 ± 5%
Tropical										
Borneo, Malaysia (This study)	6	3.66 ± 0.27	2.84 ± 0.44	0.26 ± 0.04	0.35 ± 0.05	0.75 ± 0.10	1.07 ± 0.56	1.88 ± 0.19	NA	81 ± 26%
Peninsula, Malaysia (Smith et al., 2018)		7.82 ± 4.37	3.79 ± 1.97	NA	NA	NA	NA	NA	NA	NA
Central Kalimantan, Indonesia (Stockwell et al., 2016)	35	2.86 ± 1.00	5.75 ± 1.60	0.31 ± 0.36	NA	NA	NA	NA	0.208 ± 0.059	NA
South Kalimantan, Indonesia (Stockwell et al., 2014)	3	1.39 ± 0.79	3.30 ± 0.79	1.85 ± 0.56	2.36 ± 0.03	NA	NA	NA	0.1	NA
Overall Extratropical Peat (Stockwell et al., 2014)	NA	3.38 ± 3.02	3.66 ± 2.43	0.51 ± 0.12	2.31 ± 1.46	NA	NA	NA	NA	NA
Reviews[g]										
Atmospheric Modeling (Akagi et al., 2011)	NA	10.8 ± 12.4	5.0 ± 4.93	NA	NA	1.23 ± 0.87[f]	NA	NA	NA	NA
Smoldering Boreal/Temperate		3.39 ± 6.89	3.38 ± 3.21	NA	2.31 ± 1.46	NA	NA	NA	NA	NA
Smoldering Tropical (Hu et al., 2018)		8.0 ± 3.04	5.24 ± 1.55		2.36 ± 0.03					
Peat Fire (Andreae, 2019)	3	4.2 ± 3.2	4.4 ± 1.2			1.84[f] (± 0.48 to 3.4)	NA	NA	NA	NA

[a]Data acquired from this study is highlighted in green

[b]Data acquired from Fourier Transport Infrared (FTIR) spectroscopy for this study

[c]Data acquired from the NO_x instrument upstream of the oxidation flow reactor for this study
[d]Data acquired from the NO_y instrument for this study
[e]Reported as NO_x
[f]The reported NO_x as NO was converted to NO_x as NO_2 for comparison
[g]Reviews for atmospheric modeling and emission inventory development

Table 4. Peat combustion emission factors (EFs) for $PM_{2.5}$ mass and carbon[a].

Sampling Location (Reference)	Sampling Method (No. of samples)	Modified Combustion Efficiency (MCE)	Carbon Analysis Method[b]	Average Emission Factor (g/kg)			Ratio (EF_{TC}/EF_{PM})
				$EF_{PM_{2.5}}$[c] (PM size)	EF_{OC}	EF_{EC}	
Boreal							
Odintsovo, Russia (This study)[a]	Lab (n=6, 25% FM)[d]	0.81 ± 0.03	IMPROVE_A	42.6 ± 5.2 (Fresh)[e] 40.5 ± 7.2 (Aged)[e]	25.1 ± 3.3 (Fresh)[e] 17.2 ± 2.7 (Aged)[e]	0.77 ± 0.38 (Fresh)[e] 0.69 ± 0.19 (Aged)[e]	0.61 ± 0.05 0.45 ± 0.07
Siberia (This study)[a]	Lab (n=7, 25% FM)[d]	0.85 ± 0.01	IMPROVE_A	33.9 ± 6.3 (Fresh)[e] 30.7 ± 10.2 (Aged)[e]	26.0 ± 3.4 (Fresh)[e] 18.1 ± 4.5 (Aged)[e]	0.69 ± 0.58 (Fresh)[e] 0.78 ± 0.31 (Aged)[e]	0.80 ± 0.08 0.64 ± 0.13
Pskov, Siberia (Bhattarai et al., 2018)	Lab (n=3)	NA	IMPROVE_A	7.98 ± 1.58	6.52 ± 1.4	0.02 ± 0.01	0.82
Western Siberia (Chakrabarty et al., 2016)	Lab (n=1, 25% FM)[d] (n=1, 50% FM)[d]	<0.7	IMPROVE_A	NA	17 11	0.2 0.1	NA
Neustädter Moor, Northern Germany (Iinuma et al., 2007)	Lab	0.84	VDI	44 (PM_{10})[g]	12.8	0.96	0.31
Temperate							
Northern Alaska , USA (This study)[a]	Lab (n=6, 25% FM)[d]	0.85 ± 0.02	IMPROVE_A	24.0 ± 7.6 (Fresh)[e] 24.8 ± 5.3 (Aged)[e]	17.4 ± 4.1 (Fresh)[e] 14.9 ± 3.9 (Aged)[e]	0.60 ± 0.24 (Fresh)[e] 0.55 ± 0.42 (Aged)[e]	0.77 ± 0.12 0.63 ± 0.16
Interior Alaska, USA (Chakrabarty et al., 2016)	Lab (n=1, 25% FM)[d] (n=1, 50% FM)[d]	0.7 0.7	IMPROVE_A	NA	7 4	0.1 0.2	NA
Subtropical							
Putnam County Lakebed, FL, USA (This study)[a]	Lab (n=4, 25% FM)[d]	0.65 ± 0.04	IMPROVE_A	53.1 ± 6.8 (Fresh)[e] 53.9 ± 8.3 (Aged)[e]	36.6 ± 1.9 (Fresh)[e] 37.3 ± 6.7 (Aged)[e]	1.33 ± 0.60 (Fresh)[e] 0.95 ± 0.07 (Aged)[e]	0.72 ± 0.08 0.71 ± 0.04
	Lab (n=2, 25% FM)[d]	0.67 ± 0.02		51.6 ± 7.9 (Fresh 2)[f] 48.2 ± 8.4 (Aged 2)[f]	36.6 ± 1.8 (Fresh 2)[f] 34.0 ± 8.3 (Aged 2)[f]	1.8 ± 0.61 (Fresh 2)[f] 0.99 ± 0.15 (Aged 2)[f]	0.85 ± 0.04 0.66 ± 0.10
	Lab (n=3, 60% FM)[d]	0.72 ± 0.01		35.9 ± 4.3 (Fresh 2)[f] 34.7 ± 2.6 (Aged 2)[f]	29.3 ± 2.2 (Fresh 2)[f] 22.1 ± 2.3 (Aged 2)[f]	1.00 ± 0.07 (Fresh 2)[f] 0.85 ± 0.85 (Aged 2)[f]	0.75 ± 0.11 0.72 ± 0.05
Everglades National Park, FL, USA (This study)[a]	Lab (n=7, 25% FM)[d]	0.90 ± 0.03	IMPROVE_A	23.6 ± 5.1 (Fresh)[e] 33.5 ± 11.4 (Aged)[e]	19.0 ± 4.4 (Fresh)[e] 18.8 ± 5.2 (Aged)[e]	0.78 ± 0.45 (Fresh)[e] 0.67 ± 0.30 (Aged)[e]	0.85 ± 0.15 0.60 ± 0.12

Pocosin Lakes NWR[h], NC, USA (Geron and Hays, 2013)	Field (n=3) (Feb & Aug 2008)	0.77-0.83	NA	34-55	NA	NA	NA
Green Swamp Preserve, NC, USA (Geron and Hays, 2013)	Field (n=8) (Feb 2009)	0.80-0.81	NA	44-53	NA	NA	NA
Alligator River NWR[h], NC, USA (Geron and Hays, 2013)	Field (n=8) (May 2011)	0.79-0.86[i]	NA	48-79	NA	NA	NA
Pocosin Lakes NWR[h], NC, USA (Black et al., 2016)	Lab (n=2)	0.83 ± 1.02	NIOSH	5.9 ± 6.7	4.3 ± 4.1	0.082 ± 0.091	0.74
Alligator River NWR[h], NC, USA (Black et al., 2016)	Lab (n=2)	0.86 ± 0.02	NIOSH	7.1 ± 5.6	6.3 ± 4.1	0.052 ± 0.057	0.89
Putnam County Lakebed, FL, USA (Bhattarai et al., 2018)	Lab (n=3)	NA	IMPROVE_A	6.89 ± 1.28	6.56 ± 1.10	0.04 ± 0.02	0.96
Tropical							
Borneo, Malaysia (This study)[a]	Lab (n=4, 25% FM)[d]	0.83 ± 0.03	IMPROVE_A	22.6 ± 3.1 (Fresh)[e] 22.6 ± 5.0 (Aged)[e]	18.0 ± 2.0 (Fresh)[e] 14.4 ± 1.7 (Aged)[e]	0.28 ± 0.11 (Fresh)[e] 0.29 ± 0.20 (Aged)[e]	0.81 ± 0.02 0.68 ± 0.16
Borneo, Malaysia (Bhattarai et al., 2018)	Lab (n=1)	NA	IMPROVE_A	3.9	9.62	0.1	2.4
Selangor, Malaysia (Roulston et al., 2018)	Field (n=6) (Jul/Aug 2016)	0.8-0.85	NA	28.0 ± 18.0	NA	NA	NA
Sumatra, Indonesia (Christian et al., 2003)	Lab (n=1)	Smoldering	Unspecified	NA	6.02	0.04	NA
Southern Sumatra, Indonesia (Iinuma et al., 2007)	Lab	Smoldering	VDI	33.0 (PM_{10})[g]	8	0.57	0.26
Raiu, Indonesia (Kuwata et al., 2018)	Field (June 2013) Field (Feb-Mar 2014)	NA	NA	13.0 ± 2.0 (PM_{10}) 19.0 ± 2.0 (PM_{10})	NA	NA	NA
Central Kalimantan, Indonesia (Wooster et al., 2018)	Field (n=23) (Sep/Oct 2015)	0.81 ± 0.032	NA	17.82 ± 6.86	NA	0.106 ± 0.043 (BC)[j]	NA
Central Kalimantan, Indonesia (Jayarathne et al., 2018)	Field (n=21) (Oct/Nov 2015)	0.78 ± 0.04	NIOSH	17.3 ± 6.0	12.4 ± 5.4	0.24 ± 0.1	0.73
Indonesia (location not specified) (May et al., 2014)	Lab	0.89	TOF-AMS and SP2	34.9 (PM_1)[k]	34.5 (OA)[k]	0.01 (BC)[k]	0.99

Reviews[l]							
Peatlands from tropical forest (Akagi et al., 2011)	NA	NA	NA	NA	6.23 ± 3.6	0.2 ± 0.11	NA
Smoldering	NA	NA	NA	19.2 ± 6.8	8.38 ± 4.14	0.36 ± 0.28	0.46
Boreal/Temperate	NA	NA	NA	17.3 ± 6.0	8.8 ± 4.24	0.28 ± 0.18	0.52
Smoldering Tropical (Hu et al., 2018)							
Peat fires (Andreae, 2019)	NA	NA	NA	17.3	12.4	0.19	0.73

[a]Data acquired from this study are highlighted in green

[b]The IMPROVE_A protocol reports OC and EC by Thermal/Optical reflectance (TOR, Chow et al., 2007); The NIOSH and NIOSH5040 reports OC and EC by Thermal/Optical transmittance (NIOSH, 1999); VDI is German Industrial Standard (VDI, 1999); TOF-MS: time-of-flight mass spectrometer (Drewnick et al., 2005); and Single Particle Soot Photometer (SP2, DMT Inc., Boulder, CO, USA) measures black carbon (BC) by laser-induced incandescence technique (Stephens et al., 2003).

[c]Size fraction is $PM_{2.5}$ except where otherwise noted.

[d]FM; Fuel Moisture

[e]Includes averages of all fresh and all aged emission factors (EFs) for the 25% fuel moisture (i.e., grouped Fresh 2 and Fresh 7 vs Aged 2 and Aged 7 shown in Table S7)

[f]Comparison between 25% and 60% fuel moisture content are only made with Fresh 2 vs. Aged 2 of Putnam (FL) peats.

[g]Sum of five stages of Berner Impactor with 0.05-0.14, 0.14-0.42, 0.42-1.2, 1.2-3.5, and 3.5-10 μm size ranges.

[h]National Wildlife Refuge, eastern NC

[i]From Jayarathne et al. (2018)

[j]BC by MicroAethalometer (AE 51) (Cheng et al., 2013;Wooster et al., 2018)

[k]PM_1 and organic aerosol (OA) acquired from Time-of-Flight Mass Spectrometry (TOF-MS) measurements (Drewnick et al., 2005)

[l]Reviews for atmospheric modeling and emission inventory development.

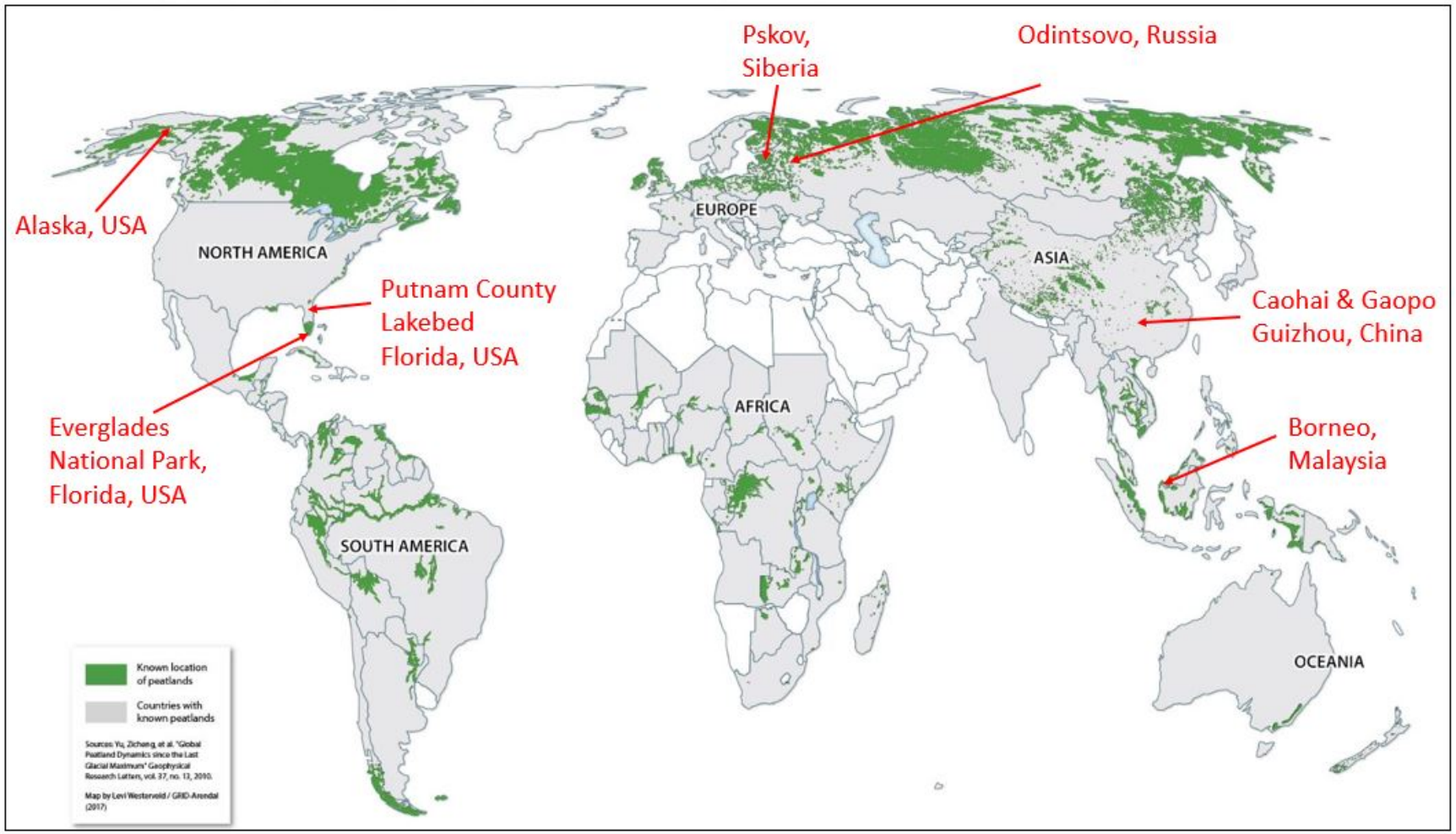

Figure 1. Global distribution of peatlands (based on Yu et al., 2010). Samples were obtained from Odintsovo, Russia; Pskov, Siberia; black spruce forest, Northern Alaska, USA; Putnam County Lakebed and Everglades National Park, Florida, USA; Caohai and Gaopo, Guizhao, China; and Borneo, Malaysia.

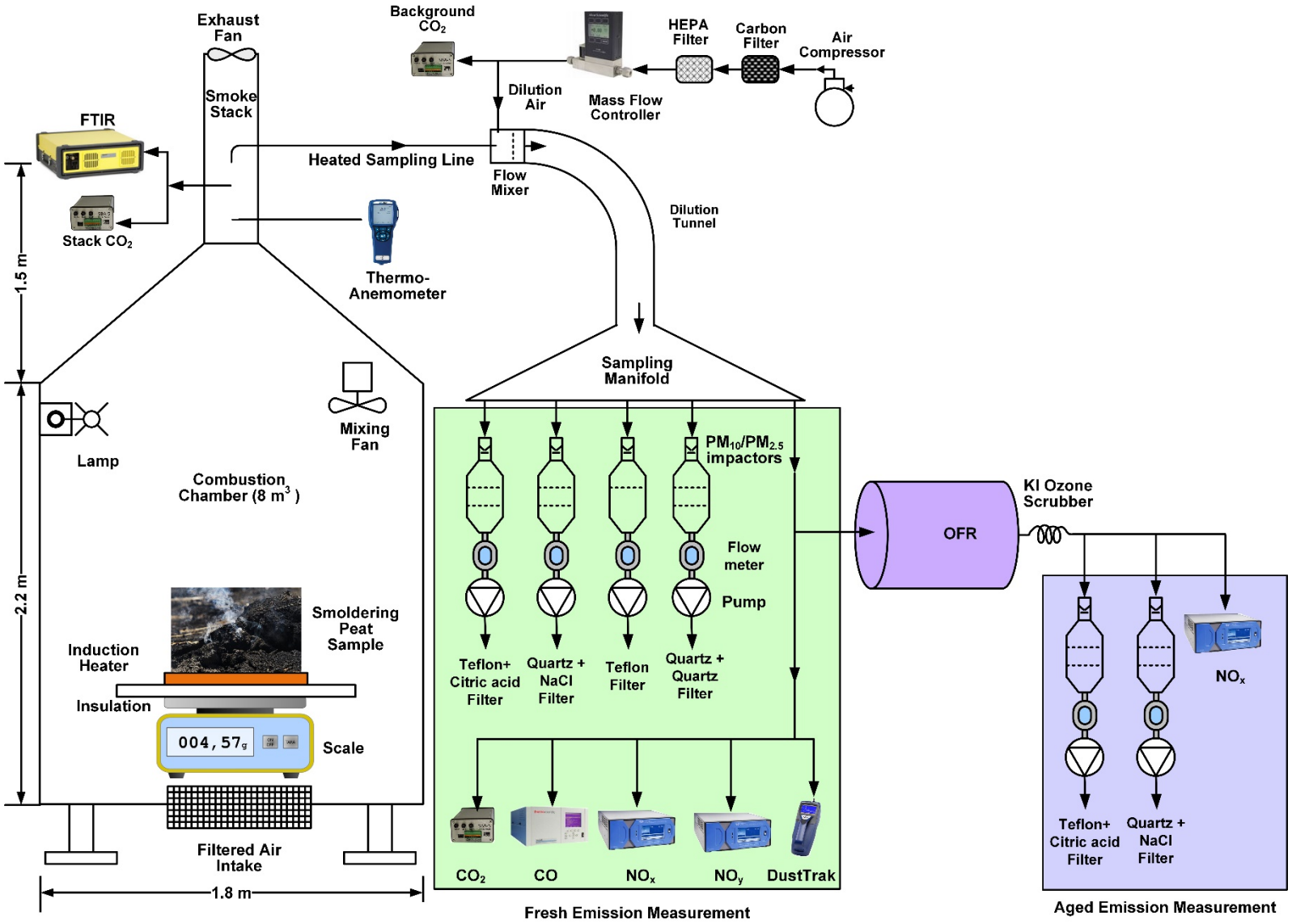

Figure 2. Configuration for peat combustion experimental set up. (FTIR: Fourier Transform Infrared Spectrometer; OFR: oxidation flow reactor; OFR lamps were operated at 2 and 3.5 volts to simulate aging of ~2 and 6.79 days, respectively).

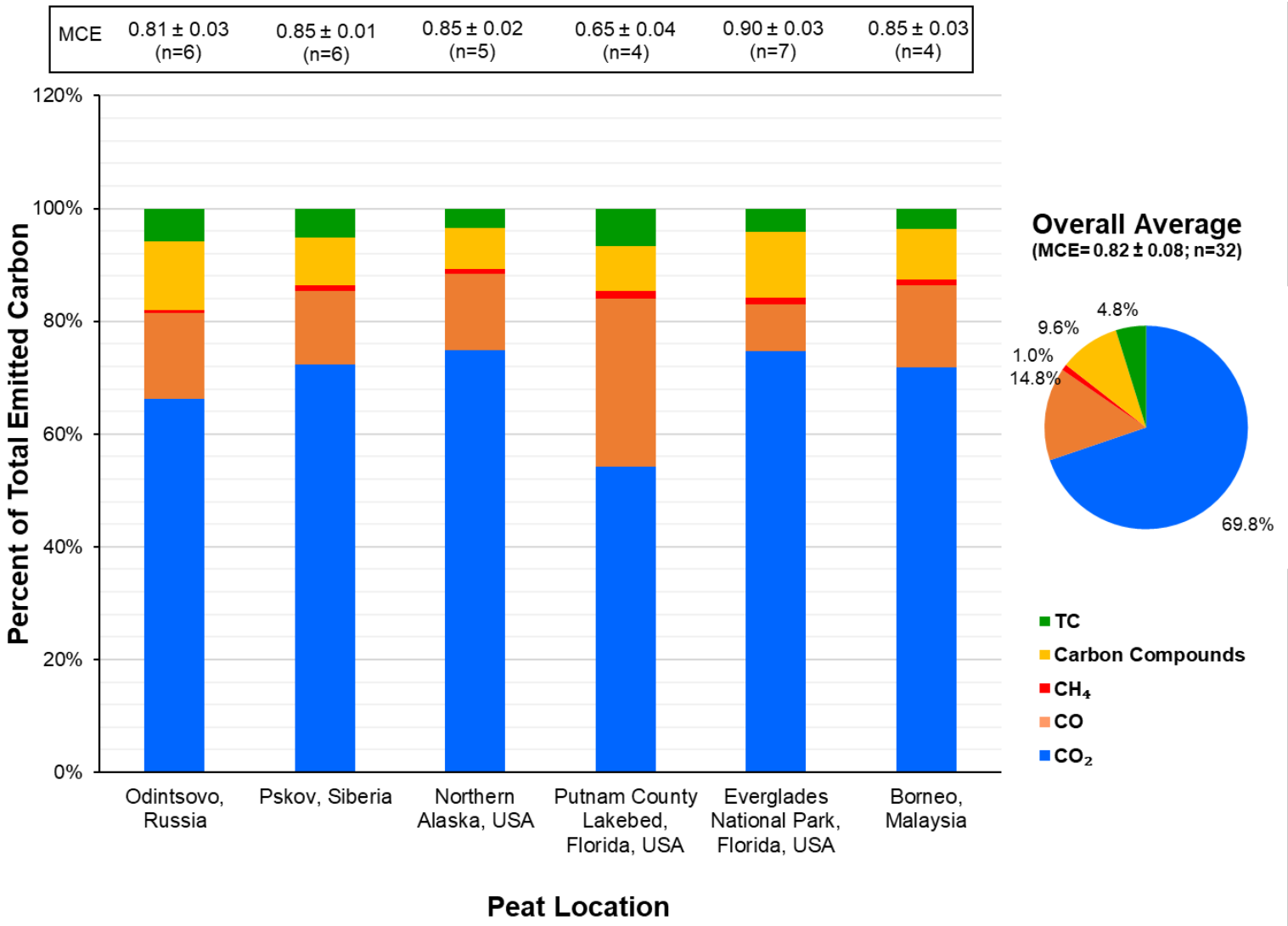

Figure 3. Average carbonaceous species abundances in total emitted carbon (the sum of carbon in CO_2, CO, CH_4, VOCs, and $PM_{2.5}$ total carbon [TC = OC + EC]). Numbers on top of the bars are average Modified Combustion Efficiencies (MCE) and the number of samples in each average. The Carbon Compounds include hydrogen cyanide (HCN), formaldehyde (CH_2O), methanol (CH_3OH), formic acid (HCOOH), carbonyl sulfide (COS), ethylene (C_2H_4), ethane (C_2H_6), acetaldehyde (C_2H_4O), ethanol (C_2H_5OH), acetic acid (CH_3COOH), propane (C_3H_8), acrolein (C_3H_4O), acetone (C_3H_6O), 3-butadiene (C_4H_6), benzene (C_6H_6), hexane (C_6H_{14}), phenol (C_6H_5OH), and chlorobenzene (C_6H_5Cl) acquired by Fourier Transfer Infrared Spectrometry.

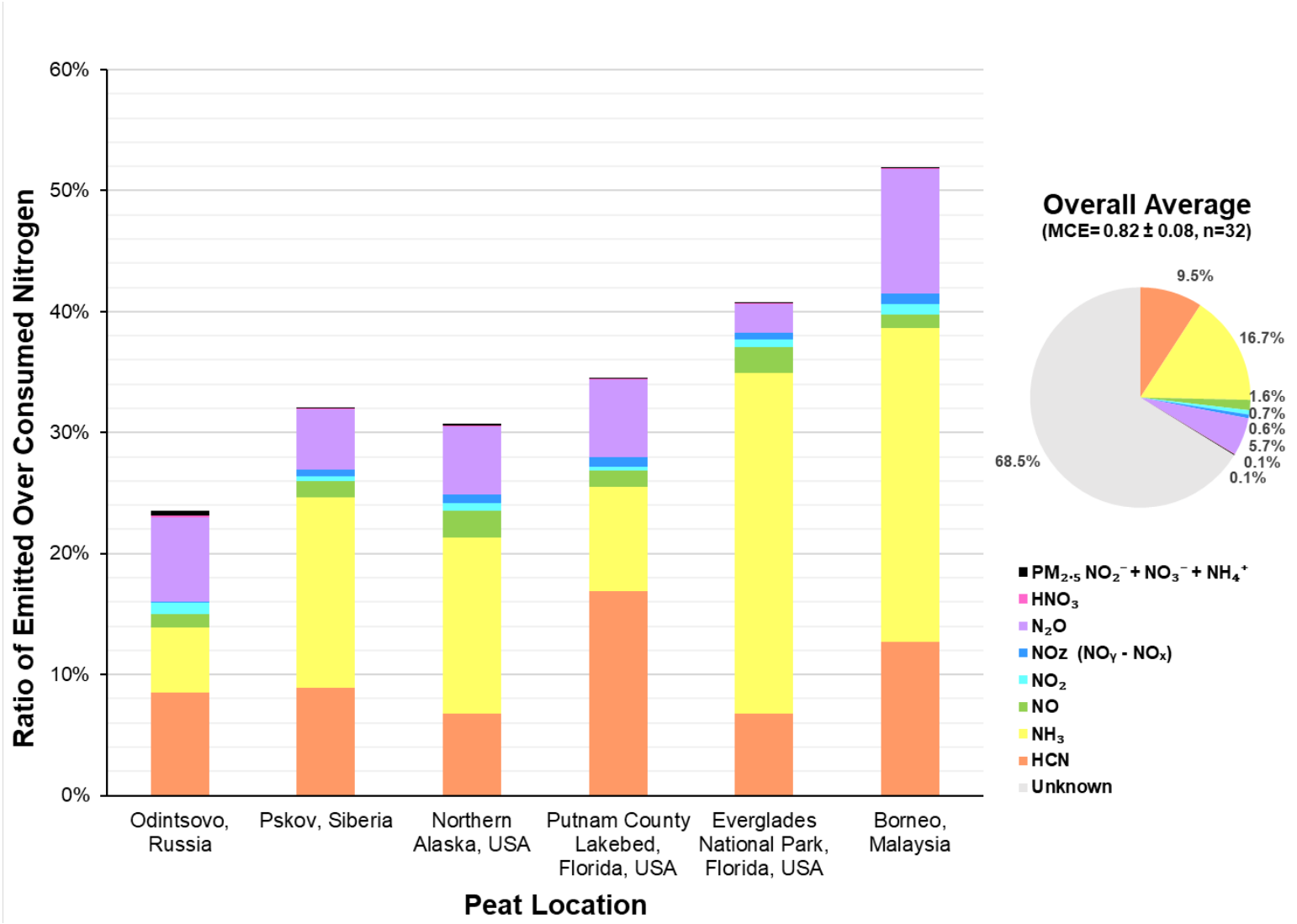

Figure 4. Ratio of emitted over consumed nitrogen for each type of peat (emitted nitrogen is the sum of nitrogen in HCN, NH_3, NO, NO_2, and NO_z [NO_y-NO_x], N_2O, HNO_3, and $PM_{2.5}$ ions [NO_2^- + NO_3^- + NH_4^+]; and the consumed nitrogen is the product of percent fuel nitrogen content and mass of fuel burned).